VALIDATION OF HALOE V20 TROPOSPHERIC WATER VAPOR USING CORRELATIVE SATELLITE DATA SETS.

A Thesis presented

By

Momodou Kaba Bah

Submitted to the Graduate College of Hampton University
In partial fulfillment of the requirements for the degree of

MASTER OF SCIENCE

May 2007

This thesis submitted by Momodou Kaba Bah in partial fulfillment of the requirements for the degree of Master of Science at Hampton University, Hampton, Virginia is hereby approved by the committee under whom the work has been completed.

Professor James M Russell III, Ph. D.
Committee Chair

Professor Patrick McCormick, Ph. D.

Professor John Anderson, Ph. D.

Donald A. Whitney, Ph. D.
Dean of the Graduate College

Date

ABSTRACT

Validation of HALOE V20 Tropospheric Water Vapor Using Correlative Satellite Data sets.

Hampton University. (May 2007)

Momodou Kaba Bah, B.S., University of Wisconsin-Oshkosh;

M.S., Hampton University

Chair of Advisory Committee: Professor James M Russell III

Abstract.

The goal of this thesis research is to validate Halogen Occultation instrument (HALOE) version twenty (V20) tropospheric water vapor using correlative satellite data sets. The correlative datasets used are the Atmospheric Infrared Sounder (AIRS), Microwave Limb Sounder (MLS), and the Stratospheric Aerosol and Gas Experiment II (SAGE II). Each selected profile was prescreened using filters recommended by the data providers, and only the best available data sets from each instrument were used for validation. First each correlative data set was independently compared with HALOE V20 using coincidence profile comparison, followed by monthly, seasonally and latitude average techniques. The mean profiles with their corresponding percent differences (% diff) and root mean squares (RMS) were computed to see if there was any dry or wet bias between HALOE and the correlative. In addition, seasonal zonal means and probability distribution functions (PDF) techniques were also used (to) independently to process each data set, and seasonally averaged to detect any relative bias between the different data sets.

Generally, HALOE showed a relative dry bias over MLS in the low and mid latitudes (~50% diff), and a slight wet bias over SAGE II in the high latitudes (~15% diff), but agreed reasonable (reasonably) well with all the correlative data sets in other places. Even though tropospheric water vapor is highly variable, an accurate and precise water vapor measurement is very important for the scientific community, because it may contribute immensely to the study of climate change and in developing better weather prediction models, and this can greatly increase our knowledge about global warming.

DEDICATION

To Isatou (Iso) and Amadou Bah, my parents who always love(ed) and believe(ed) in me.

ACKNOWLEDGEMENT

I would like to thank Professor James M. Russell III for giving me the opportunity and freedom to do this wonderful research but (and?) also providing the resistance necessary to keep me objectively analyzing the approach. I would also like to thank Dr. John Anderson who was very helpful in suggesting alternative techniques and new methods of data analysis.

In addition, I had the pleasure of interacting with graduate students: John Wrotny, Mike Hill, and Ladi Rezac, Sydney Paul, Tatyana Babakaeva, Chris Spells and Emine Bay. I am very thankful to the entire department of Center for Atmospheric Science, for all their support that made this research possible.

I am grateful to Ms. Teresa Jones for help (helping me) with the inevitable paperwork and to Mr. Aaron Smith who did everything possible to constantly keeping the network of compute(r)s needed for this research up and running.

TABLE OF CONTENTS

Chapter Page

LIST OF FIGURES

Table Page

LIST OF TABLES

Table Page

CHAPTER 1

INTRODUCTION

1.1 Importance of water vapor and the greenhouse effect

"Water vapor is the dominant greenhouse gas in the troposphere. Its greatest influences on climate forcing is in the upper troposphere, and it is generally believed that water vapor amplifies the radiative forcing associated with the anthropogenic increases in carbon dioxide" [N. Livesey, http://mls.jpl.nasagov/ products/h2o_product.php]. In addition, water vapor accounts for about 90% of the earth's greenhouse effect, which is defined as the atmospheric heating caused by solar radiation being readily transmitted inward through the earth's atmosphere but long wave radiation less readily transmitted outward, due to absorption by gases such as: (H_2O, CO_2, CH_4, NO_2) in the atmosphere. "Without the greenhouse effect(,) life on this planet would probably not exist" as we know it, because " average temperature of the Earth would be a chilly -18° Celsius, rather than the present 15° Celsius" [M. Pidwirny; http://www.physicalgeography.net/ fundamentals/7h.html].

As the temperature in the atmosphere and that at the surface of the earth increases, the atmosphere is able to hold more water vapor. Hence, more water in the sea and on land will vaporize and is carried into the atmosphere through convection and transport. Once in the atmosphere, it interacts with aerosols and other non inert gases to form clouds, acidic and non-acidic rain which determine the hydrological cycle.

In addition, "water vapor is also an important tracer for troposphere-stratospheric exchange, and as such can help in quantifying the mechanism for such an exchange" [L. W. Thomason; http://www.sage2.larc.nasa.gov/introduction]. With recent progress in satellite remote sensing techniques, it is now possible to get near global coverage of water vapor data. Hence we are getting closer to collecting sufficiently good water vapor observations to test theoretical models and monitor long-term H_2O changes.

1.2 The Climatology of Atmospheric Water Vapor and Water Vapor Trends.

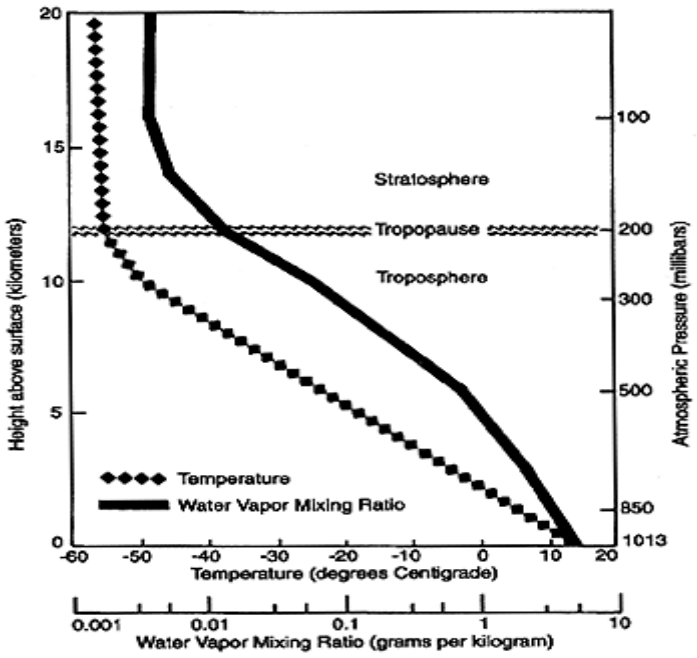

Figure 1.1 Theoretical mean vertical distributions of temperature and the water vapor mixing ratio in the atmosphere [D. Gaffen, Air Resources Laboratory, MD].

Figure 1.1 shows the theoretical mean vertical distribution of temperature and the mixing ratio of water vapor in the lower atmosphere. Water vapor rapidly decreases with height, as the atmosphere gets colder. Nearly half the total atmospheric water vapor is between sea level and about 1.5 km above sea level, while less than 5-6% of the water vapor is above 5 km, and less than 1% is in the stratosphere, nominally above 12 km [C. Russell; http://www.agu.org/sci_soc/mockler.html#starr].

Global estimate showed an increase in precipitable water during the period 1973-1990 with the largest trends in the tropics, where increases as large as 13% per decade were found. [C. Russell; http://www.agu.org/sci_soc/mockler.html#starr]. A unique research project at Boulder Colorado, which makes approximately monthly measurements of the vertical profile of water vapor with frost point hygrometer observations over a 14-year period (1981-1994) showed an increase in water vapor in the lower stratosphere over Boulder of a little less than 1% per year [S.J. Oltmans et. al., 1995].

SATELLITE DETAILS

This section consists of an introduction to the basic operating principles for each of the four instruments used in this validation, and the type of satellites on which they are mounted upon.

1.4 The Halogen Occultation Experiment (HALOE)

The Halogen Occultation Experiment (HALOE) was launched on the Upper Atmospheric Research Satellite (UARS) spacecraft September 12, 1991, and after a period of out gassing, it began science observations on October 11, 1991. The spacecraft was placed in a nominal orbit of 57° inclination and 585 km altitude. It was designed to make a systematic study of the stratosphere and provide new data on the mesosphere and thermosphere. Of the ten instruments on UARS, HALOE is one of the four that measures chemical composition. HALOE uses solar occultation to measure vertical profiles of O_3, HCl, HF, CH_4, H_2O, NO, NO_2, aerosol extinction and temperature versus pressure [Russell, et al., 1993].

1.4.1 Solar Occultation

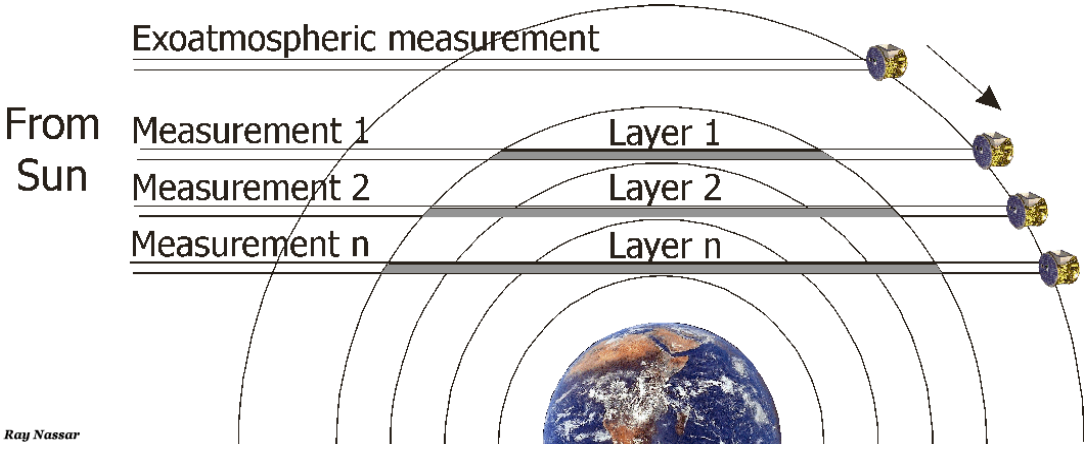

Figure 1.3 An artist depiction of solar occultation. [R. Nassar http://www.ace.uwaterloo.ca/media/ACE_onion50.gif].

Solar occultation is a technique in which sunlight being transmitted through the atmosphere is measured and then ratioed to that of a solar measurement recorded with no atmospheric attenuation (,) also called the exo-atmospheric reference phase. The absorption of sunlight being transmitted through the atmosphere is measured by keeping track of the sun position as a function of pressure at the tangent height

as shown in Fig 1.3. Subsequent measurements are carried out with increasing altitude as the sun rises or decreasing altitude as the sun sets. “During each measurement, a column is calculated using basic equations which can contain contributions from multiple atmospheric layers” and the period during which such measurements are taken is know as the atmospheric tracking phase [Russell et al., 1993]. In addition to the higher sensitivity of limb scanning over nadir viewing and the high vertical resolution that can be achieved by solar occultation, it is also virtually self-calibrating because a relative measurement is what is always being made [Russell et al., 1993]. The disadvantages are that clouds and the Earth-Sun geometry limit the coverage. In addition, sampling is poor in the tropics and measurements are made only at sunrise and sun set.

The UARS satellite typically observes 15 sunrises and 15 sunset events per day. As each event proceeds, the HALOE instrument locks onto the sun and goes through a sequence of operational modes, which can be divided into an exo-atmospheric reference phase, and an atmospheric tracking phase. During the exo-atmospheric reference phase, HALOE observes the sun above the atmosphere to measure intensity versus angle profile for the sun followed by a sequence of calibration measurements in each spectral channel. During the atmospheric tracking phase, the solar position is tracked through the atmosphere, and the atmospheric absorption is measured in each channel as a function of pressure at the tangent height [Russell et al., 1993].

The exo-atmospheric and the atmospheric tracking phases together provide the principal information needed to derive the desired atmospheric parameter profiles. “Gas mixing ratio profiles are then determined by taking the ratio of the solar intensity which has been attenuated by its passage through the atmosphere with the unattenuated intensity measured outside the atmosphere” [Hervig et al., 1993]. The instrument uses gas filter correlation radiometry for measuring HCl, HF, CH_4 and NO, and broadband filter radiometry for measuring O_3, H_2O, NO_2 and temperature as a function of pressure using a CO_2 channel. The two measurement techniques combined cover a range from 2.45 to 10.04 μm [Hervig et al., 1993].

1.4.2 Gas Filter Correlation Radiometry.

In a gas filter correlation radiometry, solar energy with transmission (τ) entering the gas correlation section of the instrument is divided into two paths by a beam splitter. The first path contains a

gas cell with a sample of the gas to be measured (e.g. HF) and the second is a vacuum path. After detection by the detectors as shown in Fig. 2.2, the output signals from each of these paths are fed into a differencing amplifier, where a differenced signal is calculated ($\Delta \mathbf{v}$). "The gas filter channel modulation signal, M, can then be formulated with considerable algebra into a succinct function " [Russell et al., 1993].

$$\mathbf{M= \Delta V/V = (G^{-} - 1)\left[(\tau_w^{-} - \tau_N^{-})/(\tau_w^{-})\right]}$$

Where: $\mathbf{G^{-}}$ = gain adjust value, $\tau_w^{-} = \left[\int_{\Delta v} N_s \tau_a F_w \, dv \Big/ \int_{\Delta v} N_s F_w \, dv\right]$,

$$\tau_N^{-} = \left[\int_{\Delta v} N_s \tau_a F_n \, dv \Big/ \int_{\Delta v} N_s F_n \, dv\right], \quad F_n = \tau_{fw}\tau_c\left[\tau_v - (\tau_g \tau_1 / (\tau_g/\tau_1)^{-})\right],$$

$$(\tau_g/\tau_1)^{-} = \left[\int_{\Delta v} N_s \tau_{fw}\tau_c\tau_1 dv \Big/ \int_{\Delta v} N_s \tau_{fw}\tau_c\tau_v dv\right]$$

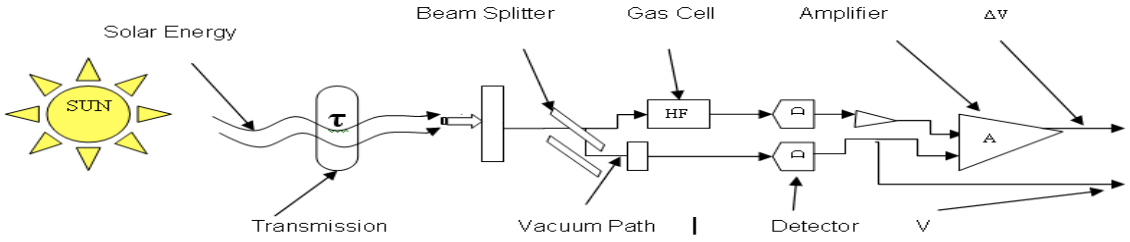

Figure 2.2 Simplified gas filter radiometry diagram.

1.4.3 Broadband Filter Radiometry

Assume we have a spectral band of width ($\Delta\upsilon$) where (υ) is a wave number, the measured output voltage ($V_{\Delta\upsilon}$), which also depends on the gas-mixing ratio (q), Atmospheric pressure (P) and Temperature (T) can be computed by using the following equation:

Responsivity factor (**C**) Solar intensity (**N**) Atmospheric transmission(ζ_a)

Inst. Aperture Area (**A**)

$$V_{\Delta\upsilon} = C A \tau \int_{\Delta\upsilon} N_s(\upsilon) * \Gamma(\upsilon) * \tau_a(\upsilon, q, P, T)\, d\upsilon$$

Measured Voltage ($V_{\Delta\upsilon}$)

Optical & electronic efficiency factor(τ) Spectral response(**Γ**)

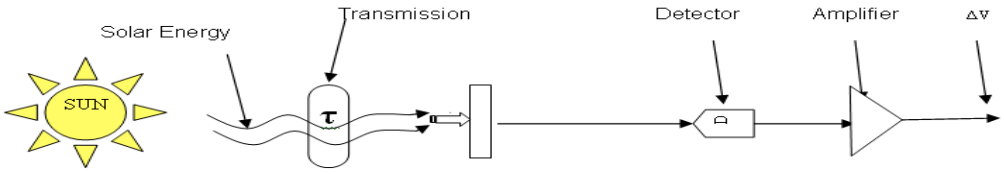

Figure 2.3 Simplified Broadband radiometry diagram.

If the sun is viewed outside the atmosphere, τ=1.0 and $V_{\Delta\upsilon} = V_{0.}$ This is called the unattenuated signal and it acts as a reference for other measurements. Since transmission is dependent on pressure (P), temperature (T) and mixing ratio (q), for a particular spectral band width ($\Delta\upsilon$) with subsequent measurements taken at different pressure levels, we can derive the average atmospheric transmission by finding the ratio between the measured signal at that point ($V_{\Delta\upsilon}$) and that of the unattenuated signal (V_0). This is done by first processing measurements for a spectral band where the gas mixing ratio is known (2.8μm CO_2 band in this case) in order to infer temperature versus pressure vertical profile. Transmission measurements are then made in other spectral bands (e.g., NO_2 H_2O or O_3) and used to infer the unknown mixing ratios [Russell et. al., 1993]. Aerosol absorption has a large effect on the radiometer measurements but signals correction methods have been developed [Hervig et al., 1993] and used successfully to derive mixing ratios.

1.4.4 Species and measurement ranges

The altitude range of the measurements extends from 15km to ~60-130km, depending on channel as shown in Table 2.1. The actual performances of the HALOE instrument exceeded its pre-lunch estimate as shown in the diagram above. The V20 water vapor is an attempt to further improve the range for the H_2O retrieval and address the crucial issue of the role of water vapor in the upper troposphere region.

Table 2.1 HALOE species, vertical resolution and corresponding altitude ranges.

Parameter	Vertical Resolution	Altitude Range
Hydrogen Chloride (HCl)	4.0 km	10 - 60 km
Hydrogen Fluoride (HF)	4.0 km	10 - 60 km
Methane (CH4)	4.0 km	15 - 75 km
Nitric Oxide (NO)	4.0 km	10 - 130 km (below 78 km)
	2.0 km	10 - 50 km
Ozone	2.0 km	10 - 85 km
Water Vapor	3.0 km	10 - 75 km
Nitrogen Dioxide (NO_2)	2.0 km	10 - 55km
Temperature	4.0 km	10 - 130 km

1.5 Atmospheric Infrared Sounder (AIRS)

AIRS (Atmospheric Infrared Sounder) is one of six instruments onboard the AQUA satellite which was launched on May 4th, 2002. It is a polar sun synchronous satellite that orbits earth at an altitude of 705.3km with an inclination of 98.2 º and 1:30pm equatorial crossing. It has an orbit period of 99 minutes and repeats a cycle after 16 days [Hagan et. al., 2004]. There are six instruments on the AQUA satellite which are: The Atmospheric Infrared Sounder (AIRS), the Advanced Microwave Sounding Unit (AMSU-A), the Humidity Sounder for Brazil (HSB), the Advanced Microwave Scanning Radiometer for EOS (AMSR-E), the Moderate Resolution Imaging Spectroradiometer (MODIS), and the Clouds and Earth's Radiant Energy System (CERES). Each has unique characteristics and capabilities and all six together form a powerful package for earth observations.

AIRS was designed to improve weather forecasting, establish connections between severe weather and climate, determine if the global water cycle is accelerating and detect the effect of greenhouse gases. The AIRS instrument measures the amount of infrared (IR) energy emitted by the atmosphere in many wavelengths. Each IR wavelength is sensitive to a particular height in the atmosphere; hence by having multiple IR detectors, each sensing a particular wavelength, a temperature profile or sounding of the atmosphere can be made. Computer programs then transforms these measurements into humidity, temperature, cloud properties and the amount of greenhouse gases. In addition, AIRS data also reveals land and sea surface temperatures with 300,000 soundings provided per day [Chahine et. al., 2003].

The heart of the instrument is a cooled (155 K) array grating spectrometer operating over the range of 3.7 – 15.4 μm and shown in Fig. 2.7. This spectrometer views the ground through a cross track rotary scan mirror which provides ±48. 95° cross tracks ground coverage along with onboard spectral and radiometric calibration sources every 2.667s. A total of 90 ground footprints are observed per scan and for each footprint, 2378 spectral samples are taken [Chahine et. al., 2003].

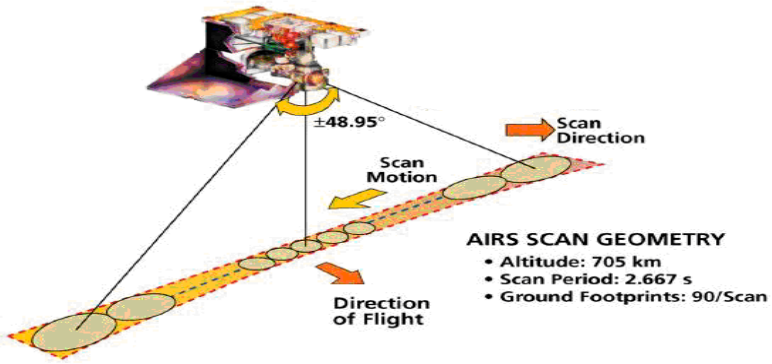

Figure 2.7 AIRS scan geometry [Chahine et. al., 2003].

AIRS IR horizontal spatial resolution is 13.5 km and the Vis/NIR spatial resolution is approximately 2.3 km. The spectrometric approach uses a grating to disperse infrared energy across arrays of high sensitive HgCdTe detectors operating at 58°K. Thick clouds act like a wall to the IR energy measured by AIRS. However, the microwave instruments onboard AQUA can see through the clouds with limited accuracy (AMSU/ HSB). Hence, data from AIRS, AMSU and HSB are carefully combined to provide highly accurate measurements in all cloud conditions, resulting in a daily global snapshot of the state of the atmosphere.

1.6 Microwave Limb Sounder (MLS)

MLS was launched on board the NASA Earth Observing System (EOS) AURA Mission on 15th July 2004 and began full up atmospheric science observations on 13th August 2004. It is an advanced follow-on to the first MLS on the Upper Atmospheric Research Satellite (UARS), which was launched on 12th September 1991 [Walters et. al., 2005].

The main EOS AURA mission is to research the composition, chemistry and dynamics of the Earth's atmosphere as well as study the ozone, air quality and climate. It is a sun-synchronous satellite orbiting at an altitude of 705km with a 98° inclination. It has a 1:45pm ascending (north-going) equator crossing time, and 98.8 minute period [M. Schwartz; http://mls.jpl.nasa.gov/data/datadocs.php].

The EOS MLS instrument provides measurements for O_3, OH, H_2O, N_2O, CO, O_3, OH, BrO, HCl, HOCl, ClO, HNO_3, HCN, and SO_2 [Walters et. al., 2005]. MLS measures naturally-occurring

microwave thermal emission from the limb (edge) of Earth's atmosphere to remotely sense vertical profiles of radiance emitted by atmospheric gases in broad spectral regions centered near 118,190,240,and 640 GHz, and 2.5THz. "An atmospheric limb scan and radiometric calibration for all bands are performed routinely every 25s. Vertical profiles are retrieved every 165 km along the sub orbital track, covering 82º S to 82º N latitude on each orbit" [Walters et. al., 2005].

1.7 Stratospheric Aerosol and Gas Experiment (SAGE II)

The SAGE II (Stratospheric Aerosol and Gas Experiment II) sensor was launched on board the Earth Radiation Budget Satellite (ERBS) on October 5th, 1984 and it continued operating until it was powered off on August 26th, 2005 [L.W. Thomason; http://www-sage2.larc.nasa.gov/instrument/]. Hence, it has one of the longest single records for a satellite mission in space. ERBS is a non-synchronous, circular orbiting satellite at an altitude of 610km with an inclination of 57° and a nodal period of 96.8 minutes [McCormick et al., 1993].

SAGE II was meant to provide near global measurements of atmospheric aerosols, ozone, NO_2, and water vapor. It uses the solar occultation technique to measure attenuated solar radiation through Earth's limb [Chiou, et al., 2004]. Just like HALOE, SAGE II normally takes 15 sunrise and 15 sunset measurements per day. It is also self-calibrating with 1km vertical resolution and covers 80°S to 80°N latitude. "The SAGE II sensor has seven channels centered at 0.385, 0.448, 0.453, 0.525, 0.600, 0.940, and 1.02μm wavelengths" [Wang et al., 2006]. Even though SAGE II was not optimally designed for taking measurements in the troposphere, the four longer wavelength channels frequently sample into the troposphere [Wang et al., 1996; Wang et al., 2001].

During its operating periods, some of the major results that came out of the SAGE II program "include illustration of the stratospheric impact of the 1991 Mount Pinatubo eruption, identification of a negative global trend in lower stratospheric ozone during the 1980s, and quantitative verification of the positive water vapor feedback in current climate models" [L.W. Thomason; http://www.sage2.larc.nasa.gov/]. In addition, SAGE II data have been used to measure the decline in the amount of stratospheric ozone over the Antarctic since the ozone hole was first noted in 1985 and "has also showed that the loss of water vapor in the region of depleted ozone was due to the formation of Polar Stratospheric Clouds (PSCs)" [Wang et. al., 2006].

CHAPTER 2

INSTRUMENT SPECIFICATIONS, FILTERS AND SAMPLE PLOTS.

This chapter describes latitude, longitude, and time track information for each of the four instruments used in our analysis. In addition, we will also discourse all the filters used in our analysis with sample overlayed plots after applying all the recommended filters.

2.1 HALOE

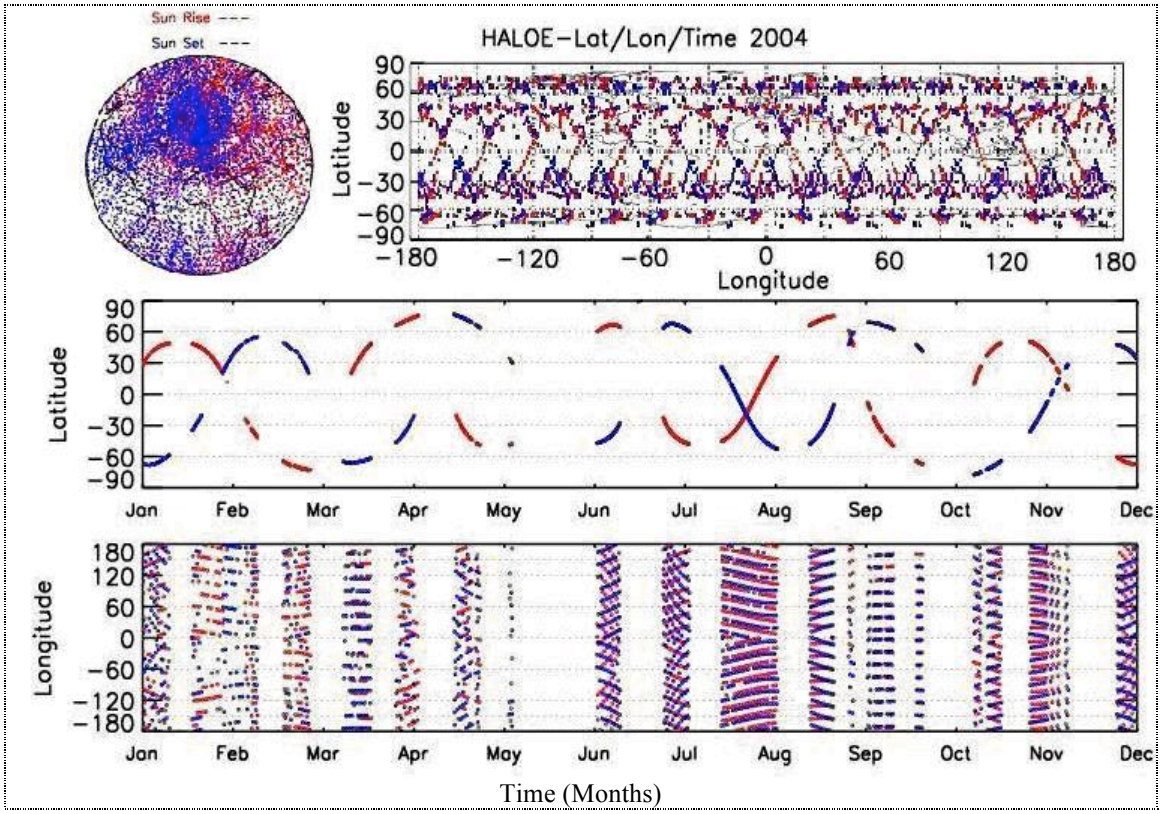

Figure 3.1 HALOE V20, Lat/Lon/Time track information show the general track and coverage for HALOE V20.

Fig. 3.1 was produced by using data from HALOE V20 water vapor for the year of 2004. Generally, latitude coverage is 80S to 80N over a course of the year. Some of the features worth noticing on the latitude/longitude plot above are, the narrow gap at ±55° latitude, and better coverage at mid latitudes than the tropics, which is one of the disadvantages of the solar occultation technique. In the middle plot (latitude

and time) we can see that HALOE's most extreme southern latitude observations occur during the spring and sometime around mid-September through early October. This period "includes the time of maximum ozone loss rate as the Antarctic ozone hole develops and recovers" [Russell et. al., 1993]. In the bottom plot, (longitude and time) we can easily see the big gaps in June and December. While some of these might be a result of filtered data, a lot of it is simply because "The earth sun line is normal or near normal to the orbit plane" [Russell et. al., 1993].

2.2 AIRS

The AURA satellite on which AIRS is mounted upon, takes only 16 days to repeat a cycle, hence it takes only few hours of following its tracks to see a pattern. Fig. 3.2 shows AIRS latitude, longitude and time plot similar to that show for HALOE in Fig. 3.1 above.

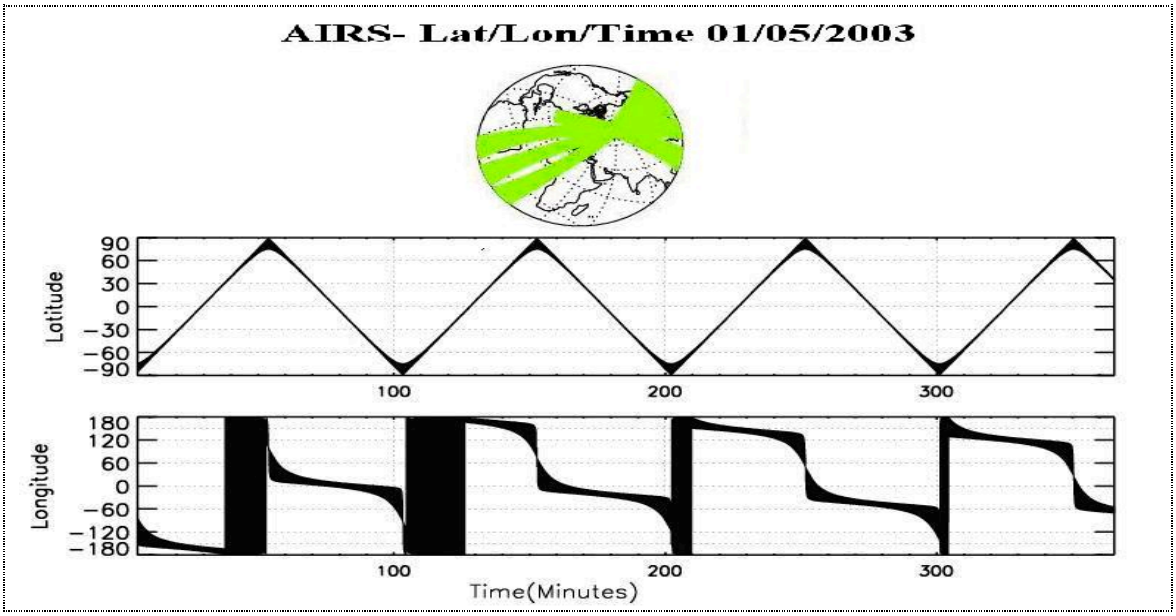

Figure 3.2 AIRS V4.0, Lat/Lon/Time track info.

Fig. 3.2 shows plots of AIRS latitude/longitude, latitude/lime and longitude/time for the first 60 out of 240 files of 01-05-2005. In the upper plot, we can clearly see that the satellite is in its 4th orbit for this particular day. It takes about 16 such orbits to cover the globe and for each orbit it passes through both poles. In the middle plot, we can easily see that it takes 100 minutes to cover the entire latitude range [Chahine et. al., 2003].

2.3 MLS

Fig. 3.3 shows MLS latitude/longitude, latitude/time and longitude plots for only the first 400 seconds (~24 minutes) of January 11th 2005.

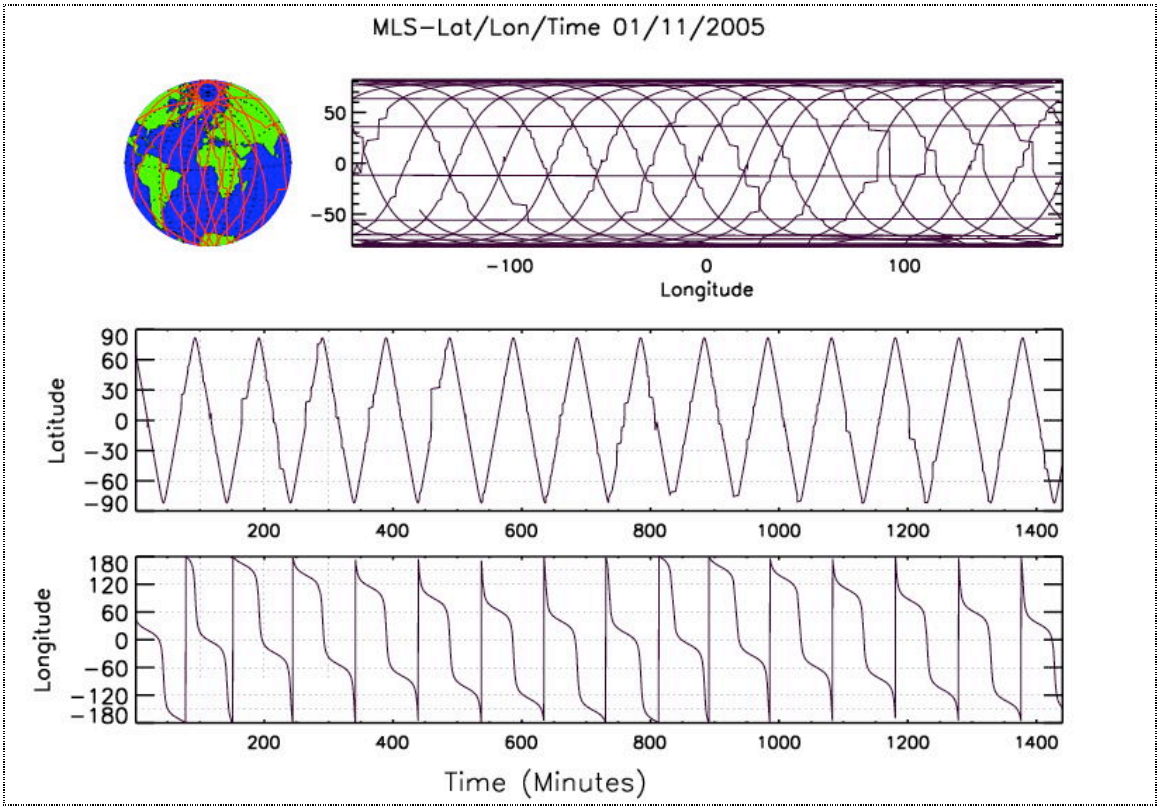

Figure 3.3 MLS V5, Lat/Lon/Time track info.

The MLS track information is very similar to AIRS shown in Figure 3.2 because they are both polar orbiting satellites and are positioned at about the same altitude. However, AIRS takes lot more measurements than MLS for each orbit. However, the MLS latitude/time and latitude/longitude tracks above suggest that the AURA satellite orbits are not as smooth as that of AQUA.

2.4 SAGE II

Fig. 3.4 shows latitude/longitude, longitude/time and longitude/time plots of SAGE II water vapor for the entire year of 2004.

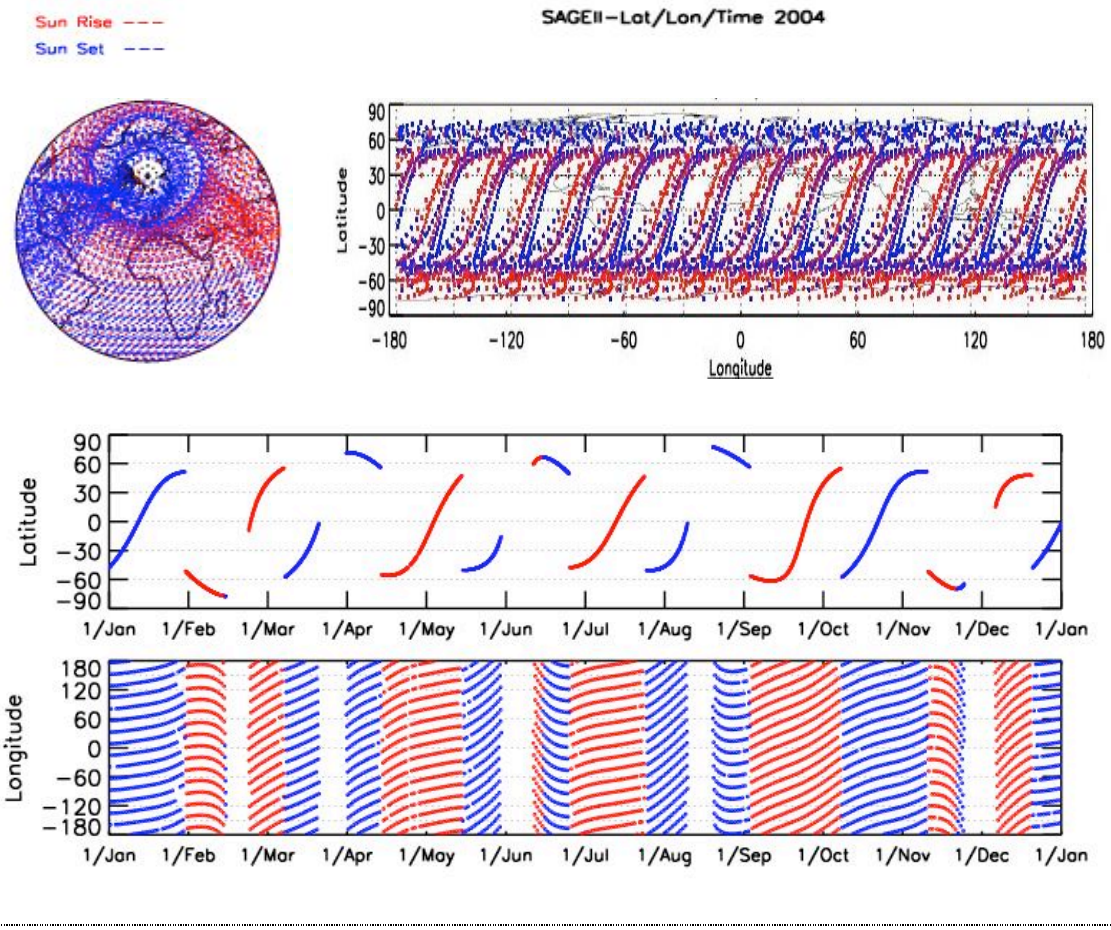

Figure 3.4 SAGE II V6.2, Lat/Lon/Time track information for 2004.

The latitude/longitude/ time tracks of SAGE II in Fig. 3.4 are very similar to that of HALOE in fig. 3.1 but different from that of AIRS (Fig. 3.2) and MLS (Fig. 3.3). Just like HALOE, SAGE II has better coverage in the mid to high latitudes than in the tropics. The main noticeable difference between HALOE and SAGE II lat/lon/time plots is that while HALOE sunset and sunrise events tend to cross particular locations within the same year, SAGE II sunrise and sunset measurements rarely overlap at any

particular location within a year. Similar plots for HALOE and SAGE II tracks in 2003 and 2005 showed the same characteristics as those in Fig.3.1 and 3.1 for 2004.

FILTERS AND DATA SELECTION

2.5.1 HALOE V20 filters

The HALOE V20 data used in this study was screened for clouds and all necessary adjustments made by the GATS, Inc. data processing team. However, to make sure that we are using only the best quality data available, we added three other filters to further screens the data and throw away only individual points that are logically invalid such as negative pressure and water vapor measurements if any. In addition, we incorporated a two sigma ($\pm 2\sigma$) filter that gets rid of data points which falls outside the 95% confidence interval. These are: the error range, out of range and the 2σ filters.

This error range filter throws away any data point with an error value greater than twice its corresponding water vapor measurement. Because individual parameters such as pressure, altitude, water vapor and temperature are reported on different grids, it is necessary to put them on the same grid before using them for comparisons. However, extrapolating all these parameters on a standard grid sometimes result into an out of range extrapolation at the boundaries which gets filtered out by the out of range filter. Finally, the 2σ filter is used to iterate thought the entire HALOE data set and throws away any particular measurement value that falls outside the 95% confidence interval.

$$\text{Standard Deviation}(\sigma) = \sqrt{\text{Variance}}$$

$$\text{Variance} = 1/(N-1) * \sum^{n-1} (x_j - \bar{x})^2$$

Where $\bar{x}$ =Mean

The main reason for adding this filter was to screen for any clouds or bad events that might have passed prescreening tests done at even though GATS Inc. An example of such a granule is shown in the bottom left plot of Fig. 3.5.

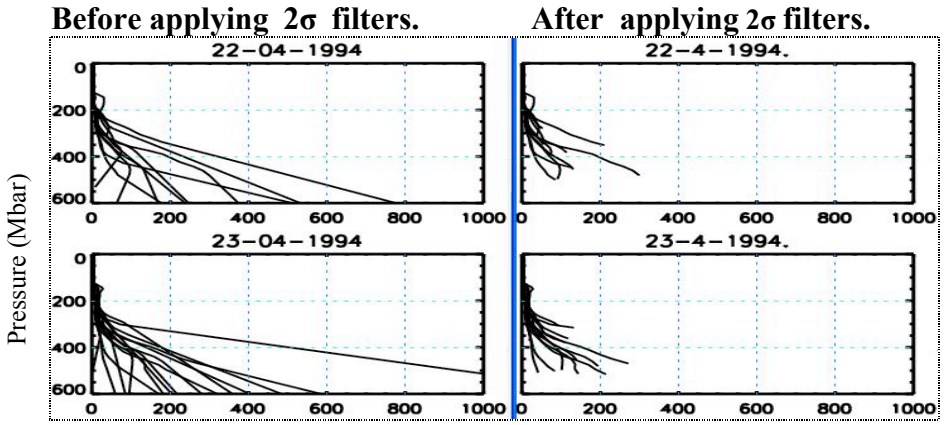

Figure 3.5 HALOE V20 before and after applying the 2σ filter.

At the time of writing this thesis, HALOE V20 data was still being processed and checked for possible improvements. An important issue that was open for discursion was coined the high HF ΔV HO_2 "Bubble", which normally appears from 10 - 15km. It was found that this was "due to rolling off the interfering/retrieved HF profile too fast with descending altitude" [E. Thompson; http://www.gats-inc.com/extract/projects_haloev20.htm]. Corrections for the high HF bubble have already been tested by the GATS Inc. data processing team and will soon be implemented in the level 2 algorithm.

2.5.2 High HF bubble filter

Fig. 3.4 shows the before and after effects of applying the High HF bubble filter to a sample HALOE V20 data. The data set used for the plot was from January 2nd to January, 4th, 2005, sunset measurement between 66ºS and 67ºS.

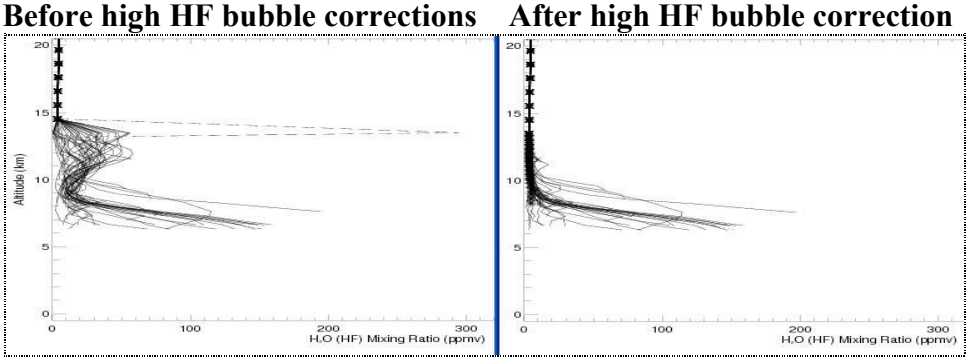

Figure 3.6 Before and after High HF filter (Courtesy of Earl Thompson, GATS)

The left hand side of Fig 3.6 shows HALOE V20 H_2O vapor before applying the high HF bubble filter and the right hand side shows the same data set after applying the high HF bubble filter. This filter made a very significant difference in the resulting output between 10 and 15km.

2.5.3 AIRS filters

AIRS data is distributed by the AIRS Data services branch of the Goddard Earth Sciences Distributed Active Archive Center (DAAC) at the Goddard Space Flight Center (GSCF) located in Greenbelt, Maryland. The recommended Version 4, AQUA final level 2 standard retrieval (L2 StdRet), (which was the latest version available at the time) was used in this validation. However, for few exceptional days where version 4 was not available at the time, the version 3 data was to compliment the missing days.

A regular day of airs L2 StdRet data is distributed into 240 different files with each file consisting of 1350 profiles and each profile was extrapolated on a standard pressure grid with 28 different levels. This yields a total of 324,000 (1350 x 240) profiles/day. The water vapor has two main filters, namely the RetQAFilter and the Qual_H2O filter. RetQAFilter is present in all Level 2 product files and "is the main quality indicator for all level 2 products in the swath data field". By selecting only the profiles with RetQAFilter = 0, yields "the highest quality retrievals and within the class of record type which has been validated" [Fetzer et. al., 2005]. This means such a profile had passed all the possible tests done by the MLS data processing team. However the amount of data set will be greatly reduced if only such profiles are selected. The before and after effect of applying the RetQAFilter are shown in Fig. 3.7 below.

Before RetQAFilter After RetQAFilter

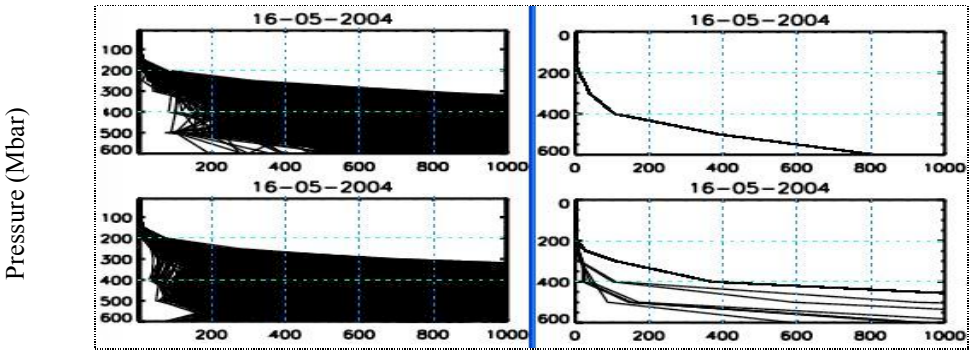

Figure 3.7 Before and after applying the RetQAFilter.

Fig 3.7 shows the effect of applying the RetQAFilter on a randomly chosen data. Due to the large amount of data lost, using this flag was not a good enough alternative, because getting close enough coincidences with the HALOE V20 at (±4hours, ±2° latitude and ±4° longitude) feasible. However the more moderate Qual_H2O filter, which is the flag for only water vapor fields along with the Press_valid_bottom flag when applied to the MLS L2 StdRet as recommend by the AIRS data processing team, yield much better results than the RetQAFilter. Fig 3.8 shows the before and after effect of apply the Qual_H2O and the Press_valid_bottom flags to a sample MLS L2 StdRet.???

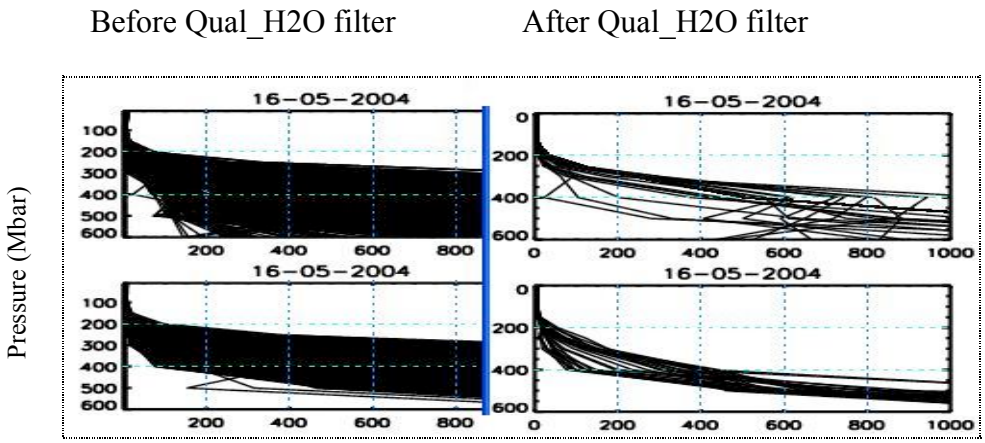

Figure 3.8 Before and after applying the Qual_H2O filter

Fig. 3.8 shows the effect of apply the Qual_H2O and the Press_valid_bottom filter on the same data set used in figure 3.7. Even though majority of the profiles gets thrown out here too, it still leaves a lot more profiles for comparison with HALOE than the RetQAFilter shown in Fig. 3.7.

MLS filters

The standard and diagnostic EOS MLS products are stored in the level 2 Geophysical Product (L2GP). "These are standard HDF-EOS (version 5) files containing swaths in the Aura-wide standard format" [Walters et. al., 2005]. The files are produces on a one-day granularity (midnight to midnight, universal time), and each file has an associated swath file with it. In addition every profile of each product also has a quality and a status flag. The recommended filters by the EOS MLS data processing team for the level 2 Version 1.5 data are: (1) the Quality control, (2) Status and (3) L2gpPrecission filters.

2.6.1 Quality and Status filters and L2gpPrecission filter

The Quality filters, "gives a measure of the quality of the product based on the fit achieved by the level 2 algorithms to the relevant radiances" [Livesey et. al., 2005]. Larger values (5 to 8) generally indicate good radiance fit while values closer to 0 indicates poorer radiance fits and therefore less trustworthy data. "The minimum value of Quality (Threshold) recommended for water vapor is 5.0"(citation?) which is what we used for the Quality filter.

The Status metric filter is a 32 bit integer that acts as a bit field containing several "flags". For example an odd value in the first bit indicates that the profile is not recommended for use in any scientific study [Livesey et. al., 2005].

The L2gpPrecission filter is a flag that is either positive or negative. A negative value in this flag indicates that the instrument and/or the algorithms have failed to provide useful information for that point. Hence only data points with a positive L2gpPrecission flag are recommended for scientific research [Livesey et. al, 2005].

Before L2gpPrecission filter After L2gpPrecission filter

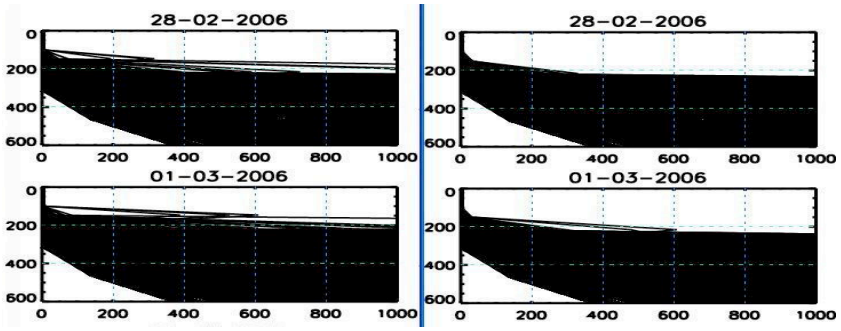

Figure 3.9 Before and after applying the L2gpPrecission filter.

SAGE II Data

The SAGE II version 6.2 (V6.2) data, which was the latest available at the time of writing this thesis, had bit-flags which (that?) acted as a filter. The primary change to the algorithm from V6.1 to V6.2 had a rectification made to the "altitude registration problem and also dealt with the improvement of the water vapor product [L.W. Thomason; http://www-sage2.larc.nasa.gov/instrument/].

2.7.1 Bit flag filter

SAGE II V6.2 date came with bit flags for each data point measurement. If the 7th and 8th bits are both 1, it indicates that there is a cloud at that particular altitude. Fig 3.10 shows the before and after effect of applying this bit flag filter to a sample SAGE II V6.2 data for 08-07-1991 and 09-07-1991.

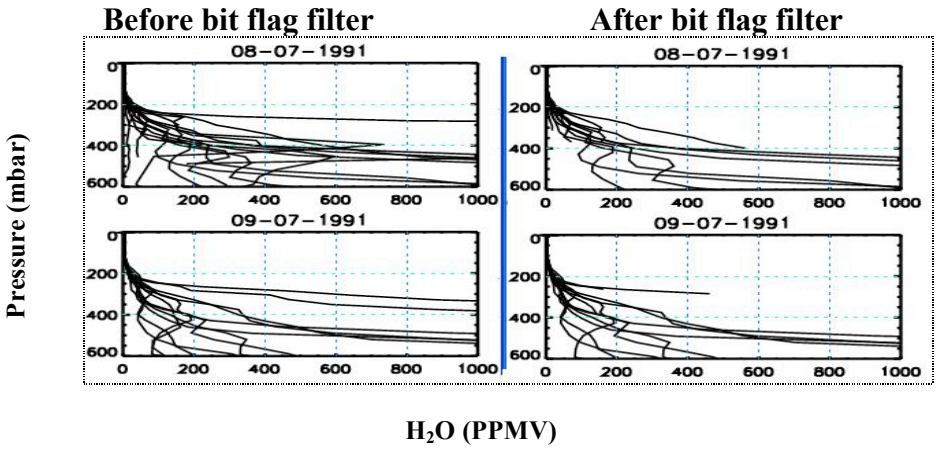

Figure 3.10 Before and after applying the bit flag filter.

SPECTRAL LINE PLOTS

This section comprises of overlayed spectral line plots for each of the four data sets after applying all the recommended filters by the respective team of data provides.

2.8.1 HALOE V20

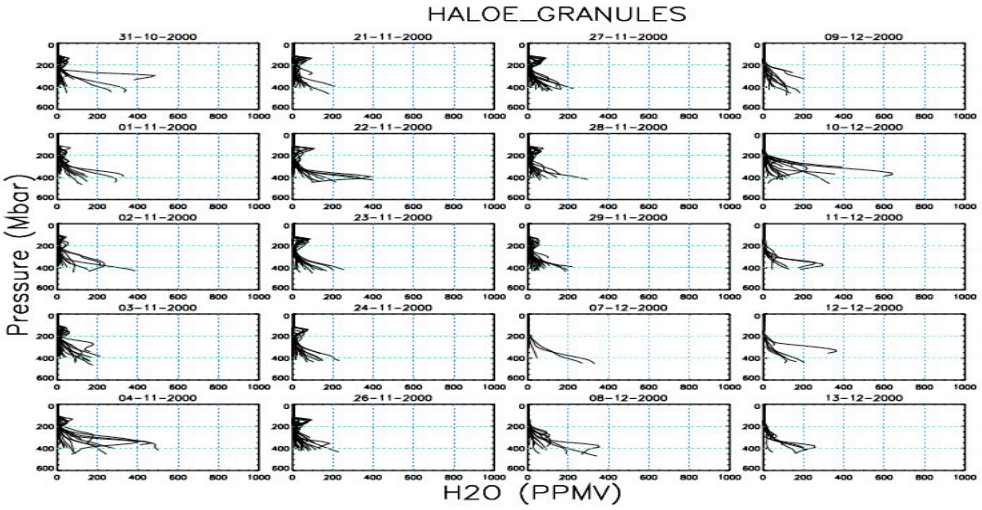

(a)

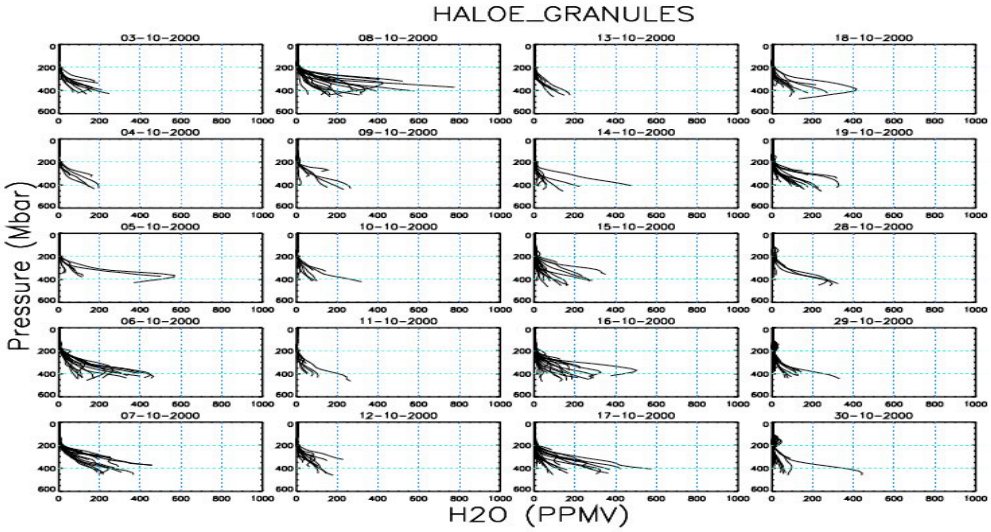

(b)

Figure 3.11a (top) and Figure 3.11b (bottom). Spectral HALOE profiles plots for particular days.

The High HF bobble can be seen in fig.3.11a while the bending of some profiles at the bottom can be seen in fig. 3.11b. Generally, tropospheric water vapor increases rapidly with decrease in altitude. As the amount of water vapor tends to increase so does the variability between measurements also increase as shown in Fig 3.11a and Fig. 3.11b.

2.8.2 AIRS L2 stdRet.

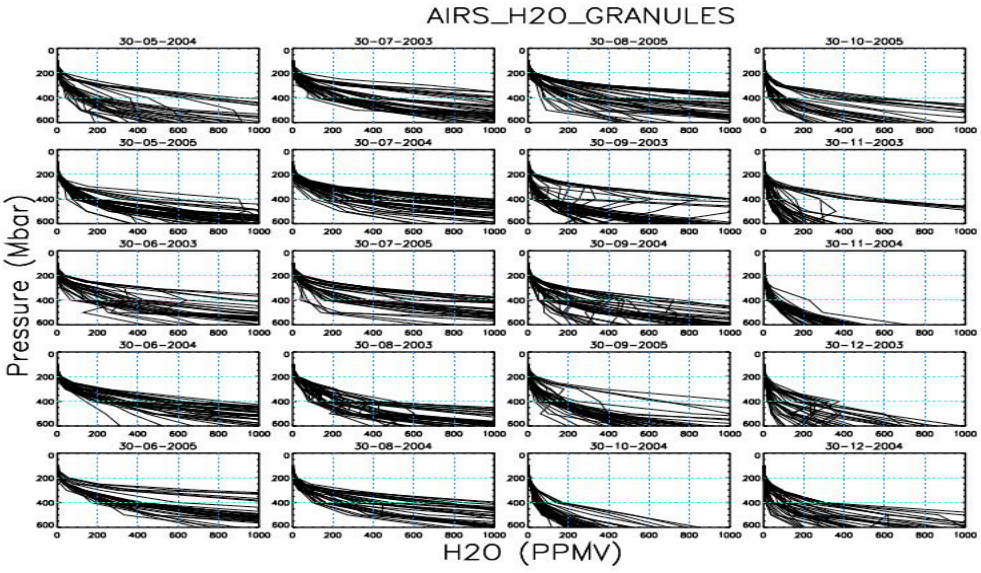

(a)

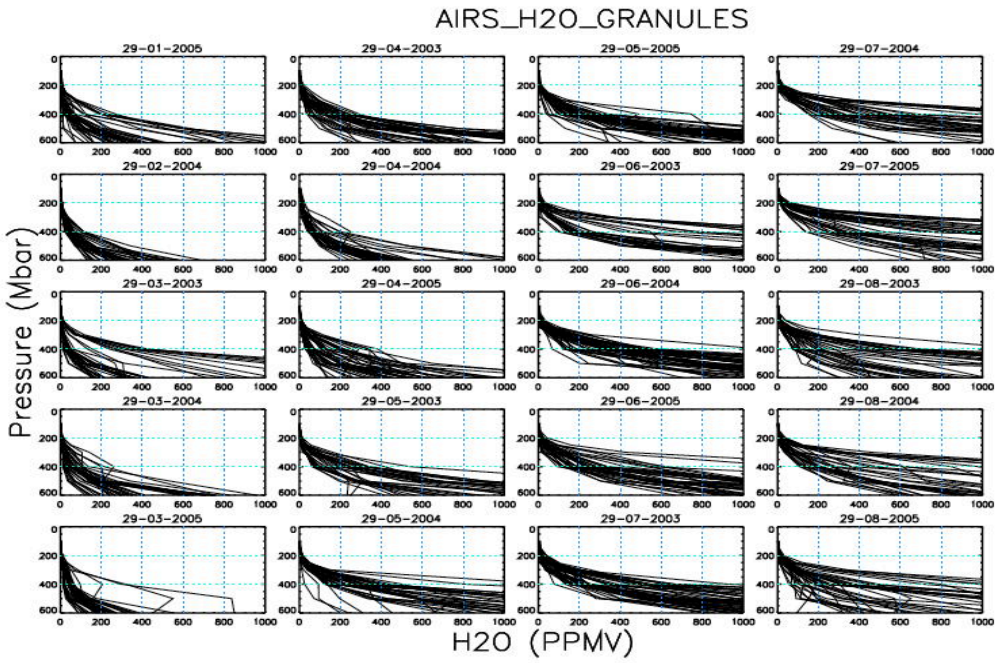

(b)

Figure 3.12a (top) and Figure 3.12b (bottom). Spectral AIRS profiles plots for particular days.

AIRS measurements tend to penetrate deeper in the lower troposphere but variability between measurements also increases rapidly as water vapor values increases in the troposphere.

2.8.3 MLS L2gp

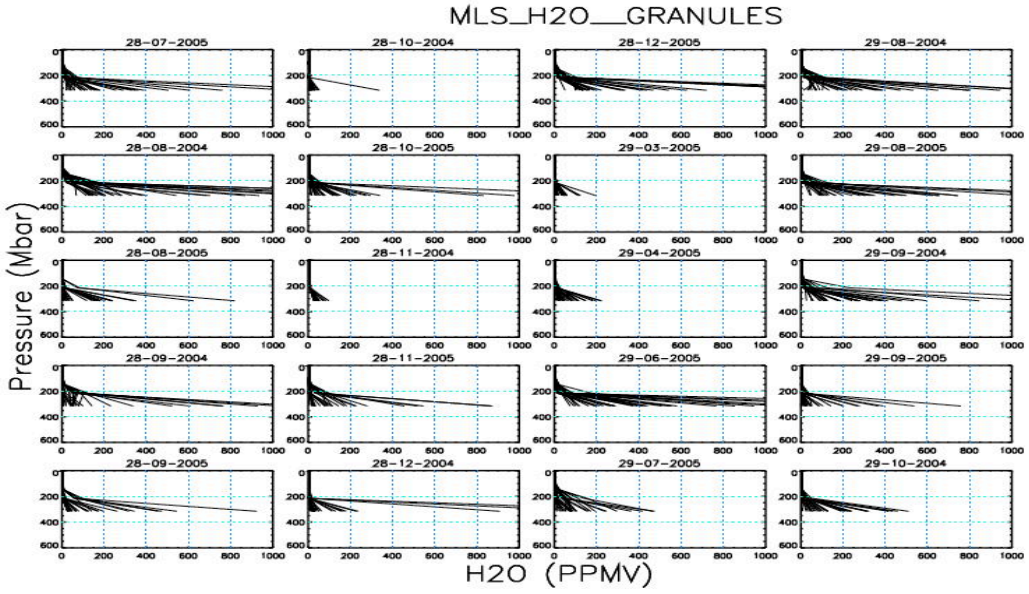

(a)

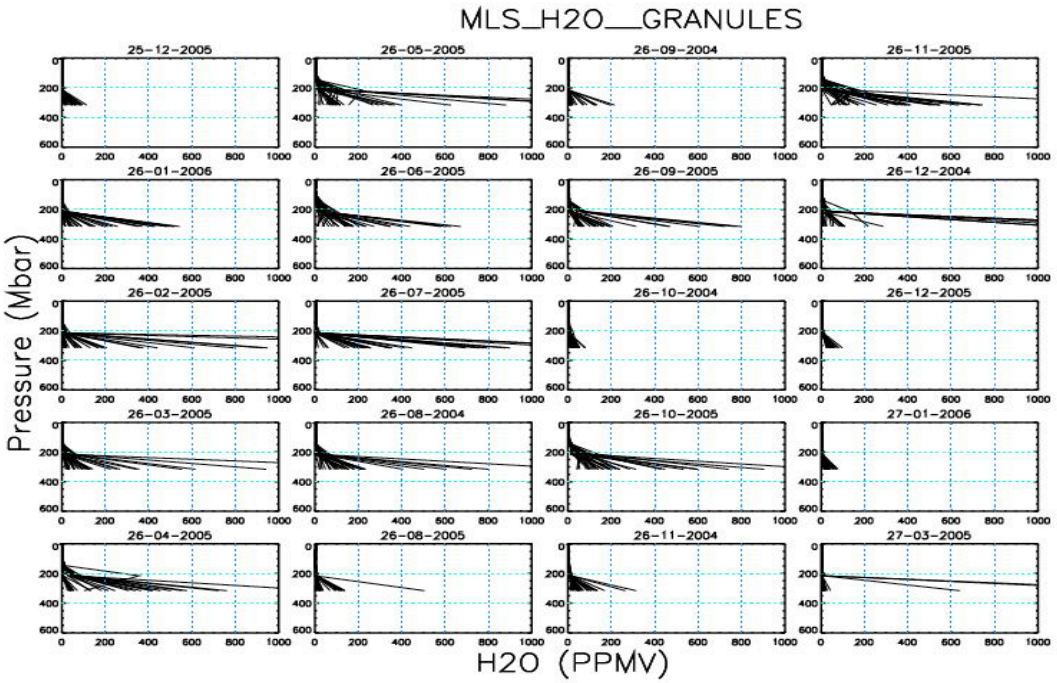

(b)

Figure 3.13a (top) and Figure 3.13b (bottom). Spectral MLS profiles plots for randomly chosen days.

MLS also shows huge variability within its own measurements. In addition, the pressure_valid_bottom filter that was recommended by the MLS data processing team puts a lower cap to the data at (~300mbar).

2.8.4 SAGE II

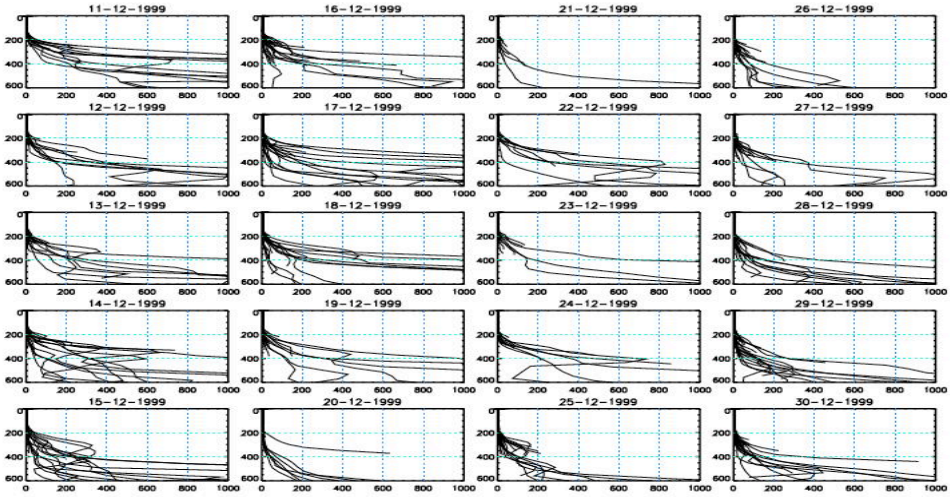

(a)

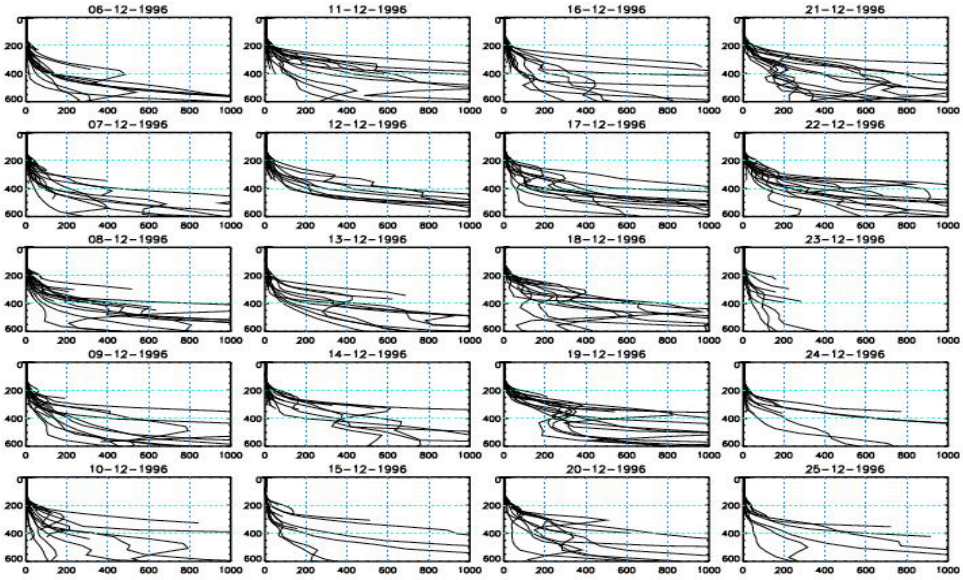

(b)

Figure 3.14a (top) Figure 3.14b (bottom). Spectral SAGE II profiles plots for particular days.

The SAGE II spectral line plots show in Fig 2.14a and 2.14b looks very similar to those of HALOE (Fig. 3.11a and 3.11b). However, the SAGE II measurements do penetrate deeper into the troposphere than HALOE V20.

CHAPTER 3

SINGLE PROFILE AND MONTHLY AVERAGE COMPARISONS

This chapter describes the spectral and monthly average comparisons between HALOE V20 and each correlative (AIRS, MLS, SAGE II) water vapor dataset. Since tropospheric water vapor is highly variable, it is very important to make sure that water vapor measurements being compared are as close to each other as possible in terms of latitude, longitude(,) and time. The coincidence criteria for all the comparisons shown in this chapter were set to [±2° latitude, ±12° longitude, and ±12hours]. Each individual HALOE profile with a given latitude, longitude and time, was independently compared to each of the correlative data sets for any possible coincidence. If multiple coincidences are found in the

correlative data for a given HALOE profile, the correlative measurement with the closest latitude and time gets selected as the best match.

3.1 Single profile comparisons

For each pair of coincidences between HALOE and the correlative water vapor profile, percent differences relative to HALOE at each given altitude are computed. Single profile plots of such comparison and their corresponding percent differences (% diff) are shown in Fig. 3.1a. The horizontal green line in each plot represents the tropopause height. The date of measurement, with mean latitude and longitudes where measurements occurred are printed in the header for each pair of events. In addition, the mean latitude, longitude and time differences for each pair of events are printed for each plot.

$$\textbf{\% diff} = [(H - C)/(H + C)]*200$$

Where: H= HALOE, and C= correlative data.

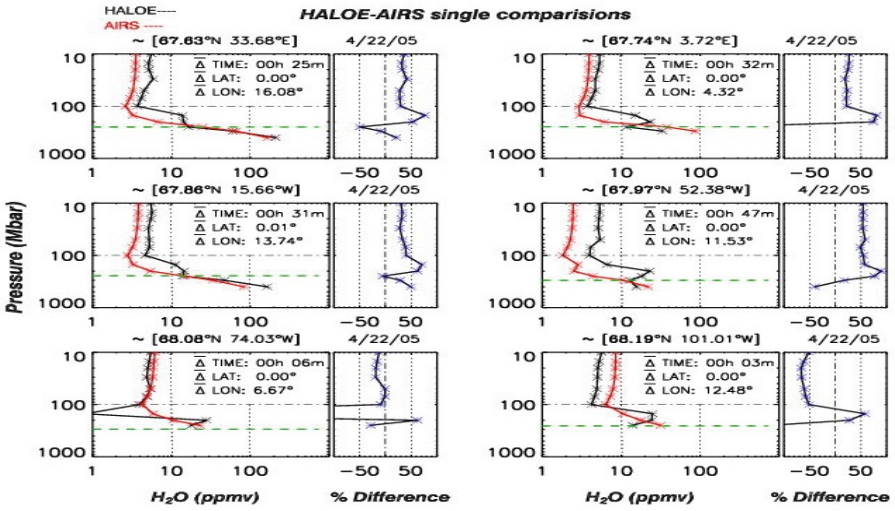

(a)

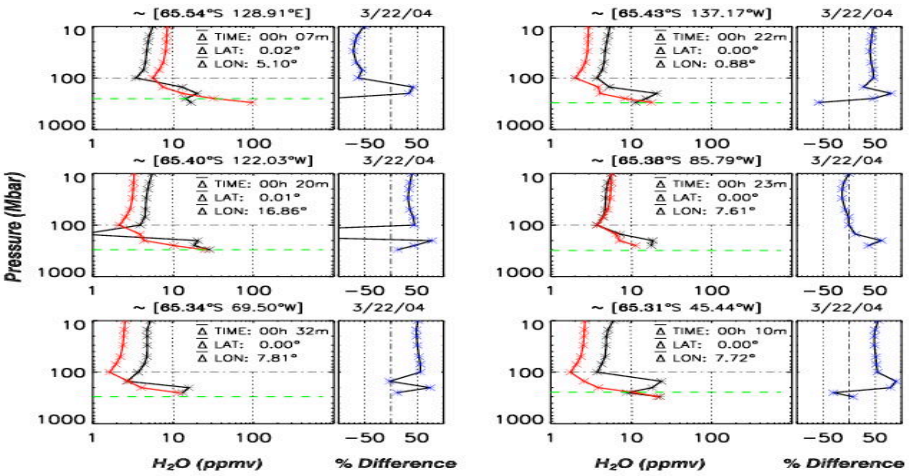

(b)

Figure 3.1: HALOE and AIRS single profile coincidence plots. (a) HALOE-AIRS coincidence plots for April-22-2005 at ~68°N, and between (101°W - 74°W). (b) HALOE-AIRS coincidence plots March-22-2004 at ~65°S, and between (137°W - 128°E).

Generally, HALOE and AIRS agree within ±50% difference as shown in Fig. 3.1a, and 3.1b. HALOE is wet bias over AIRS in the upper left plot of Fig. 3.1a, and dry bias over AIRS in the upper left plot of Fig. 3.1b.

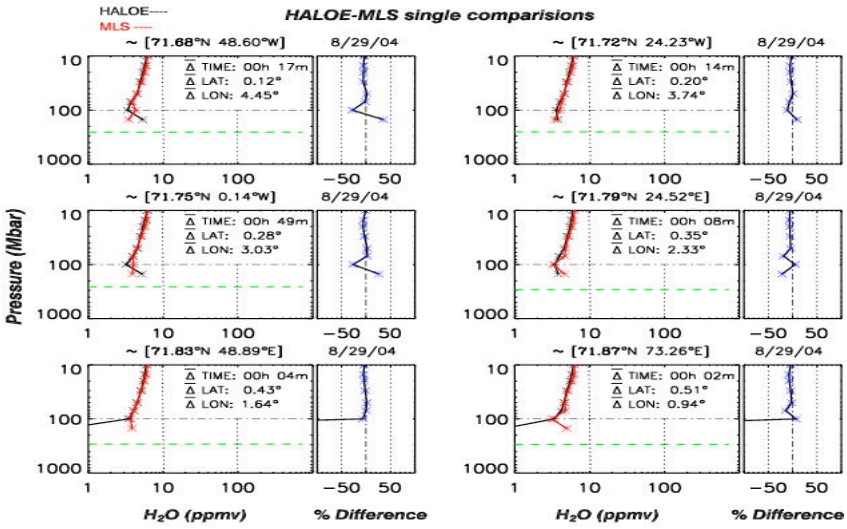

(a)

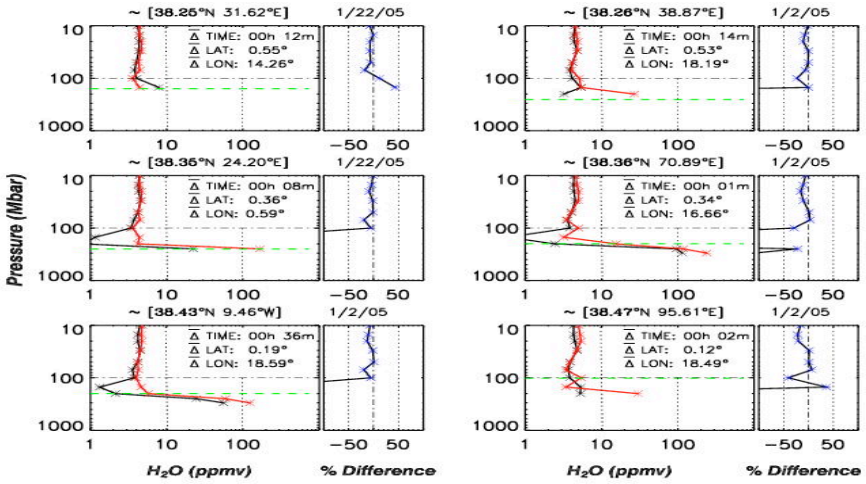

(b)

Figure 3.2: HALOE and MLS single profile coincidence plots. (a) HALOE-MLS coincidence plots for August-29-2004 at ~71°N, and between (48°W - 73°W). (b) HALOE-MLS coincidence plots January-02-2005 at ~38°N, and between (9°W - 95°E).

HALOE and MLS agree mostly within ±10% difference for pressure ranges between 10 and 100mbar. Hence, these plot(s) looks a little better than the HALOE-AIRS shown in Fig. 3.1a, and 3.1b. However, it is worth noting that the MLS data sets used in our comparisons tend to stop at about 300mbar. This is due to the effect of applying the recommended filters by the MLS data processing team. In addition, MLS takes lot more measurements per day than SAGE II. Hence there are much chances of finding very close coincidences between HALOE and MLS than between HALOE and SAGE II. Despite the seasonal differences the comparisons looks very similar.

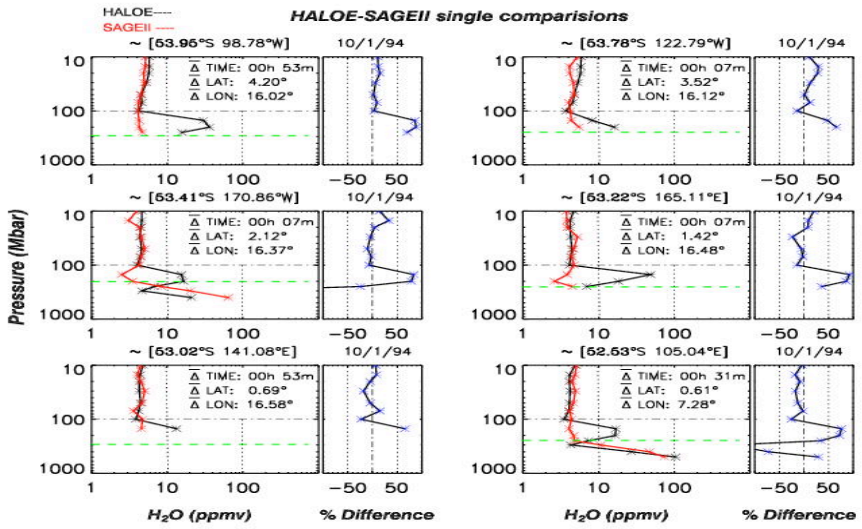

(a)

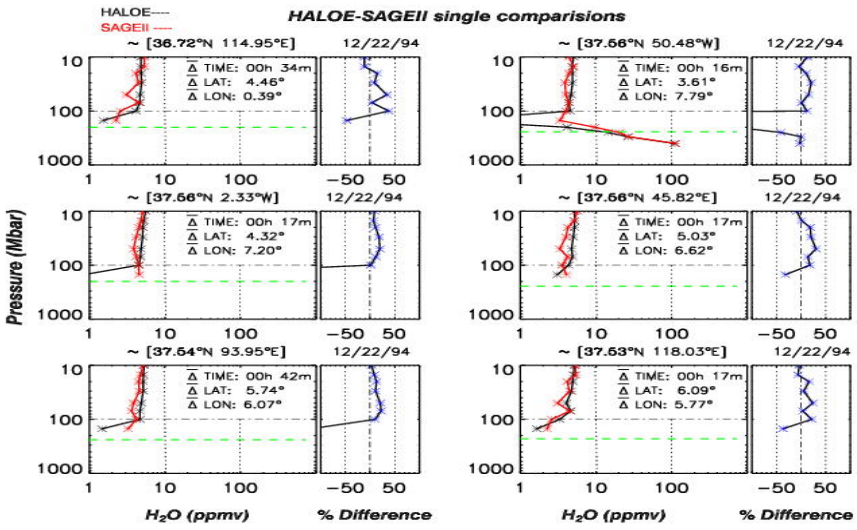

(b)

Figure 3.3: HALOE and SAGE II single profile coincidence plots. (a) HALOE-SAGE II coincidence plots for October-01-1994 at ~63°S, and between (170°W - 165°E). (b) HALOE-SAGE II coincidence plots December-22nd-1994 at ~37°N, and between (50°W - 114°E).

From Fig. 3.3a and 3.3b, it can be deduced that HALOE and SAGE II agree within ±15% difference between 10 and 100mbar. In Fig. 3.3a, HALOE is on average wet bias over SAGE II between 100 and 300mbar while in Fig. 3.3b, HALOE is dry bias over SAGE II between 100 and 300mbar.

4.2 Monthly average comparisons

This section comprises of monthly averaged comparisons for HALOE-AIRS, HALOE-MLS and HALOE-SAGE II. Similar comparisons between correlative datasets such as: AIRS-MLS, and AIRS-SAGE II are shown in appendix B.

For each month of HALOE V20 water vapor data, a subset of the same month from a given correlative dataset is obtained. These smaller sub datasets are then compared for any possible coincidences using a coincidence criterion of [±2° latitude, ±12° longitude, and ±12hours]. The average profile of all the coincidences found for each instrument are separately computed and plotted, along with their corresponding root mean squares (RMS), and mean of the differences from each pair of coincidence (MEAN) as shown in Fig 3.3a.

Each figure in this section consists of four separate plots. A thick vertical line in the middle of the figure separates the two hemispheres with northern hemisphere on the left and southern hemisphere on the right. For each hemisphere, the top plot shows overlaid spectral lines of the profiles that went into computing the averages, with the number of measurements from each instrument and the covered latitude range printed in the plot. The bottom plot shows the mean profile from each instrument on the left with the mean of the differences (MEAN) and the RMS on the right. The average (latitude, longitude and time) differences for the entire set of coincidences are computed and printed in the bottom left plot. The asterisk (*) represents points where data is actually available and the horizontal colored lines on each asterisk represents the sigma values for that measurement. The green horizontal dashed line represents the average trapopause height, and the yellow shaded regions represent the traupopause range.

It is important to note that, these comparisons are only one to one, meaning for each unique HALOE profile, there is only one unique corresponding coincidence selected from the correlative dataset. Hence in cases where multiple coincidences are found for a particular HALOE profile, the one with closest latitude and time gets chosen.

Plot Key:
Instrument 1: Inst 1
Instrument 2: Inst 2
Latitude: Lat
Longitude: Lon
Root Mean Square: RMS
Average difference: Δ (with a bad on top)
Southern Hemisphere: [SH]
Northern Hemisphere: [NH]

4.2.1 HALOE and AIRS monthly comparisons

Generally, HALOE-AIRS monthly comparisons are very promising. These comparisons showed that: HALOE is sometimes wet bias over AIRS, and sometimes (it has?) dry bias. However most evidence seems to favor an over all dry bias of HALOE over AIRS. Fig 4.2a, 4.2b, and 4.3c are representative sample plots covering the low, mid and high latitudes.

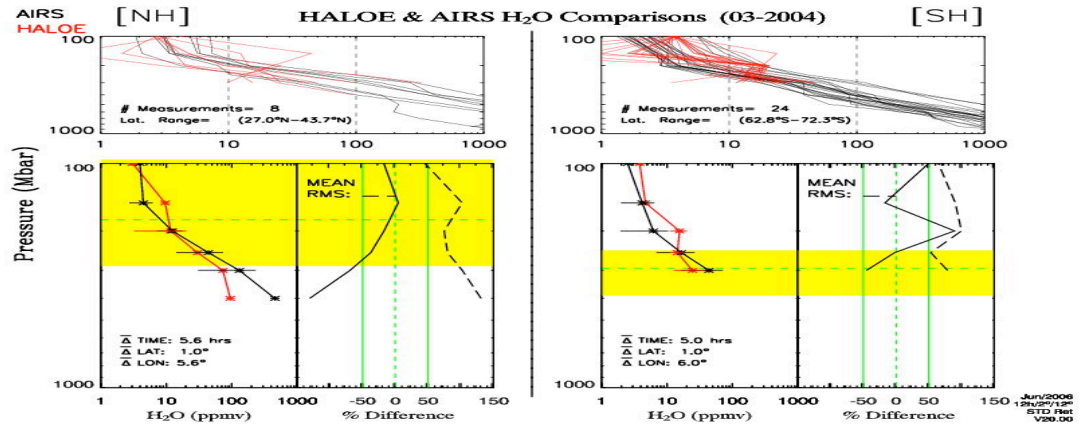

(a)

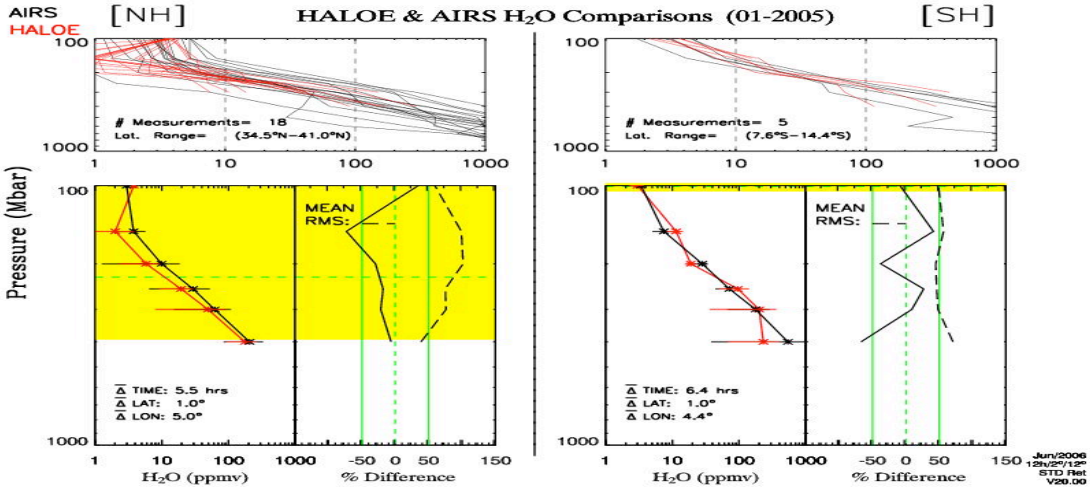

(b)

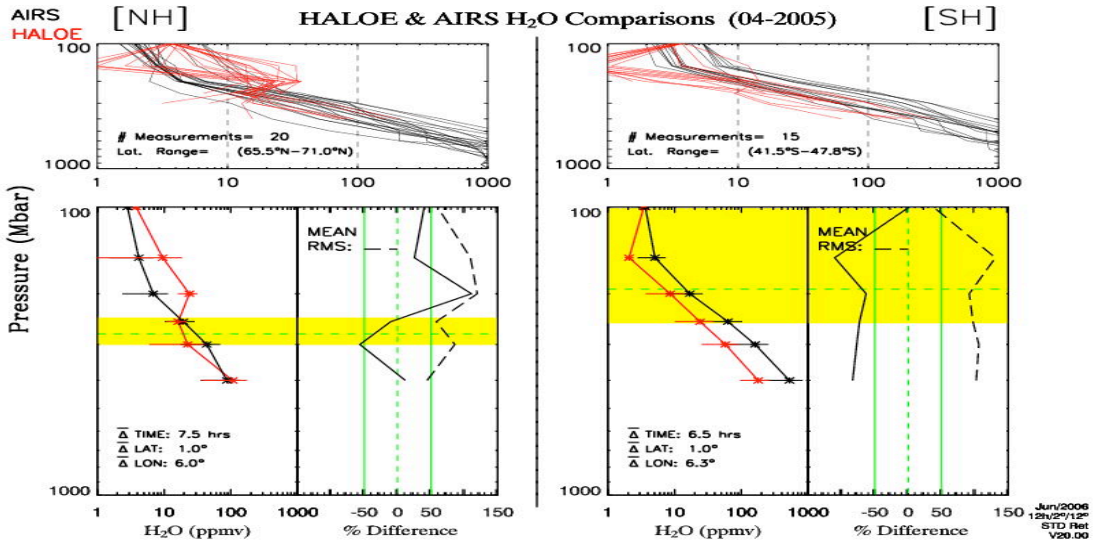

(c)

Figure: 4.4 HALOE-AIRS monthly hemispheric spectral plots, with mean and RMS % differences. (a) 05-2003, (b) 03-2004, and (c) 04-2005. In Fig. 4.4a, HALOE is generally dry bias over AIRS in the NH, but wet bias in the SH. In Fig. 4.4b, HALOE is dry bias over AIRS in the NH, but the SH shows no significant

over all bias. Fig 4.4c shows that HALOE is wet bias over AIRS between 100-280mbar and dry bias between 280-400mbar in the NH. However HALOE is dry bias over AIRS in the SH.

4.2.2 HALOE and MLS

Similar to the HALOE- AIRS plots shown in section 4.2.1, HALOE- MLS has cases where HALOE is wet bias as well as dry bias relative to AIRS. However, HALOE- MLS comparisons do as not yield as much coincidences as HALOE-AIRS because AIRS takes more measurements than AIRS. Fig 4.5a, 4.5b and 4.5c were selected as representative sample plots covering the low, mid and high latitudes.

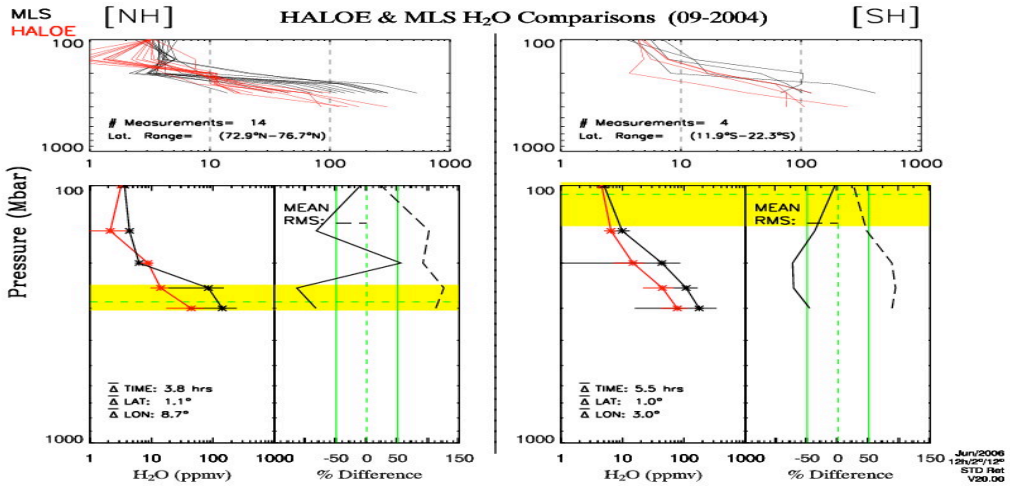

(a)

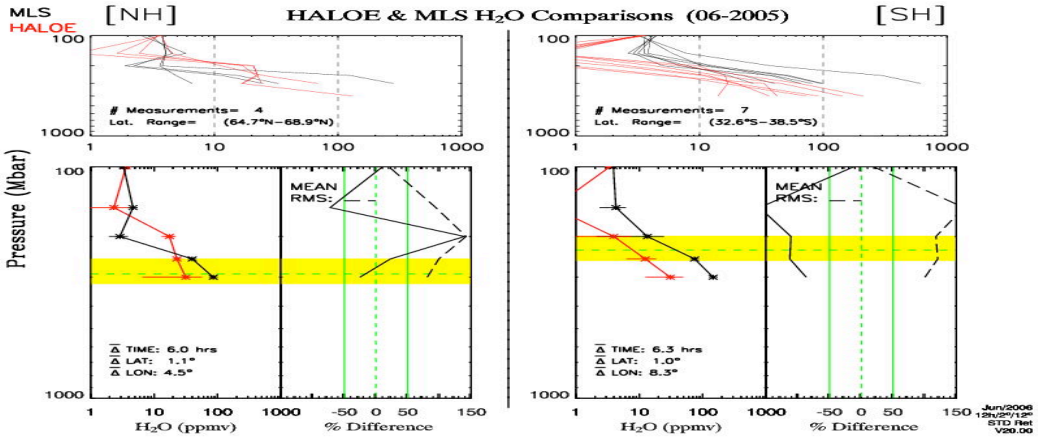

(b)

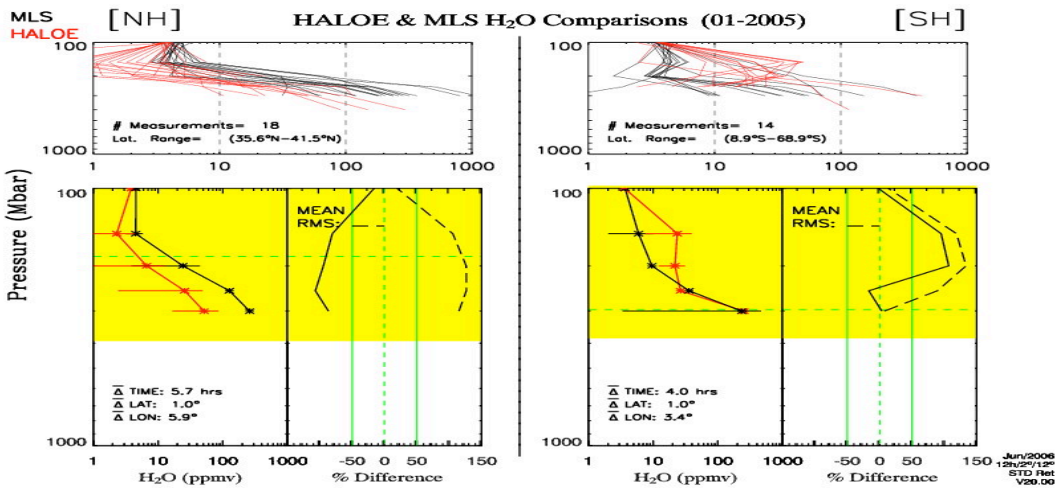

(c)

Figure: 4.5 HALOE - MLS monthly hemispheric spectral plots, with mean and RMS % differences for (a) 09-2004, (b) 06-2005 and (c) 01-2005. In Fig. 4.5a HALOE is slightly wet bias in the high latitudes NH, but dry bias in the low latitudes SH. In Fig. 4.5b HALOE is again slightly wet bias in the high latitudes NH, and dry bias in the mid latitudes SH. In Fig. 4.5c HALOE is dry bias in the mid latitudes NH but wet bias in the low and mid latitudes combined.

4.2.3 HALOE and SAGE II

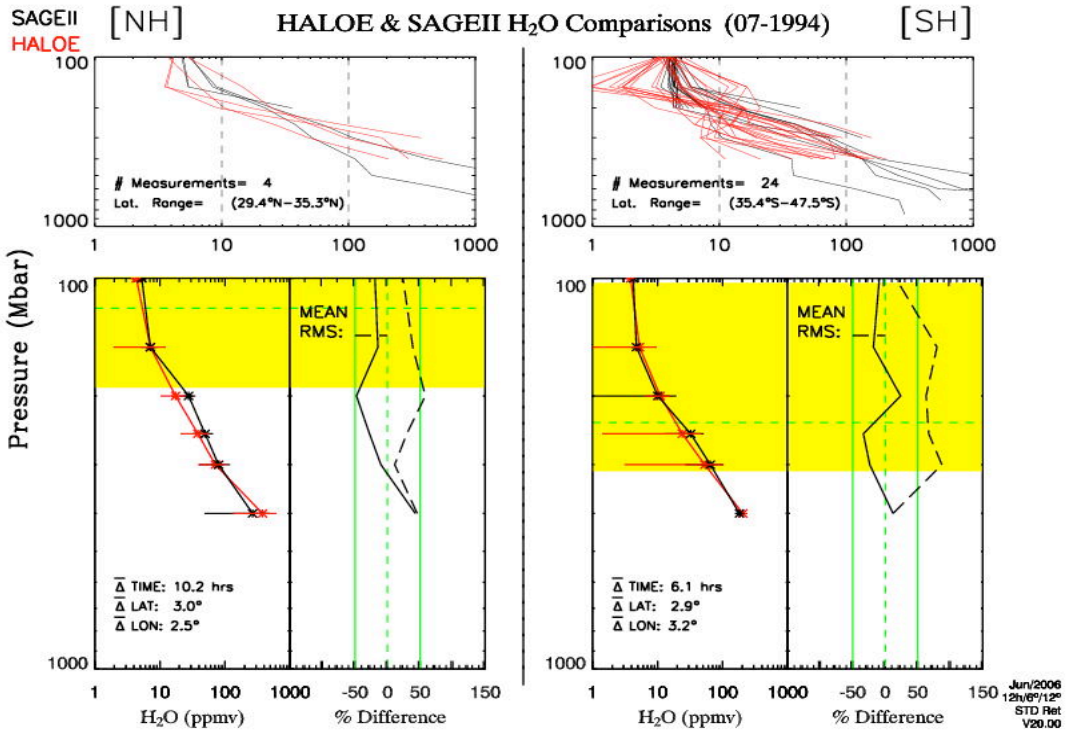

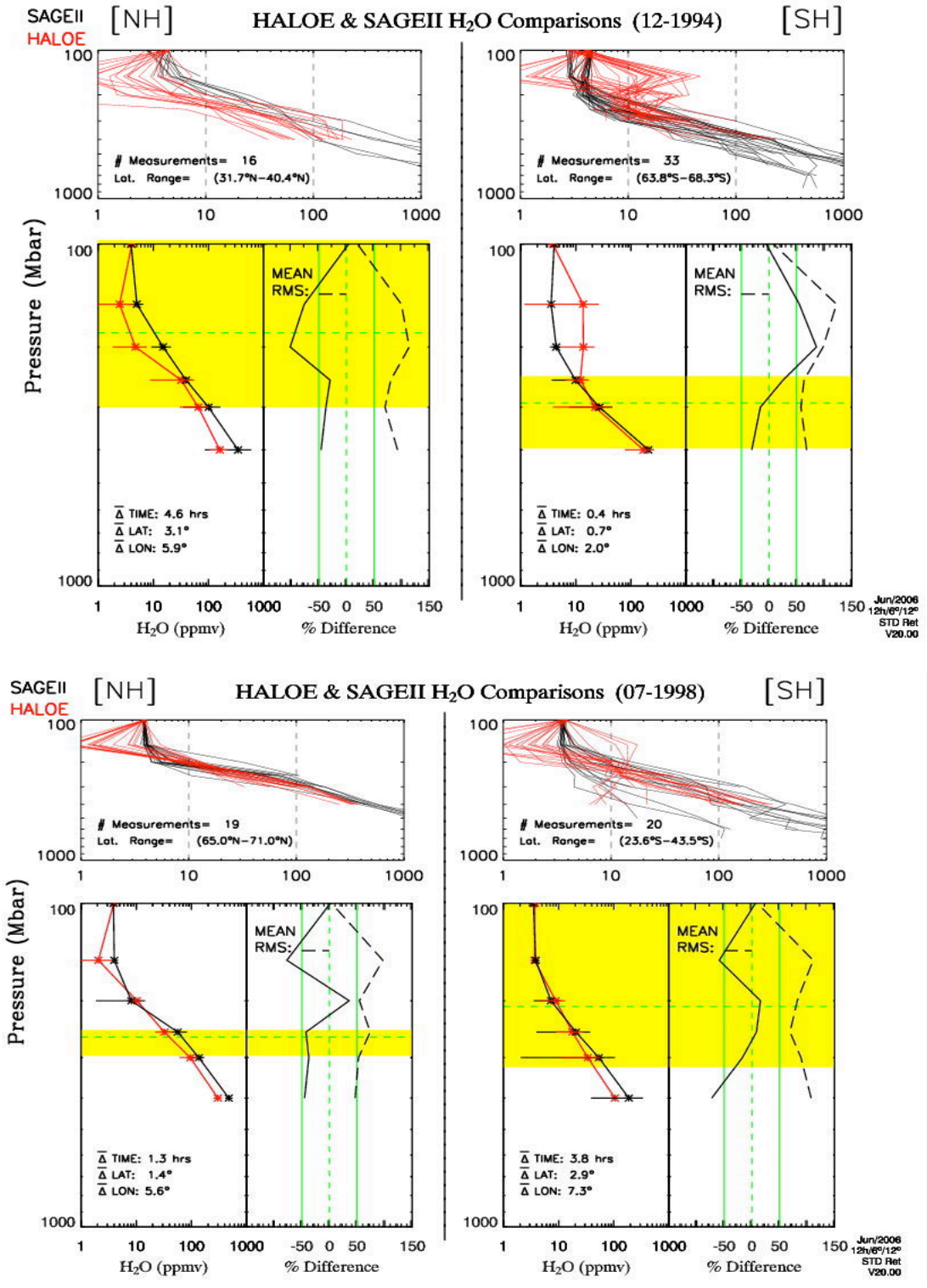

Figure: 4.6q HALOE/SAGE II monthly hemispheric spectral plots, with mean and RMS % differences for 08-2004.

4.2.4 Plot analysis

HALOE and AIRS seems to agree reasonably well except for few cases as shown above. Generally, the percent differences tend to fall within ±50. While this sounds very significant, it is actually very promising considering the natural variability of lower atmospheric water vapor and the limited data set we have from our solar occulting instruments. No consistent correlation was found between dry or wet biasness versus latitude or longitude for these comparisons. However, when all the data is averaged, HALOE shows a slight dry biasness over AIRS. Details of such biasness between instruments will be further discoursed in the following chapter.

HALOE and MLS comparisons shown above are very promising as well. The statistical values are similar to HALOE and AIRS except we tend to generally have more coincidences for HALOE - AIRS than we did for HALOE - MLS. This is simply because AIRS has a better horizontal resolution than MLS, and hence takes lots more measurements daily. The high HF bubble in the HALOE V20 retrieval can be seen in some of the plots such as figure 4.2b southern Hemisphere [SH]. Hence we hope to have even better statistics once the HF filter is in cooperated into the V20 retrieval algorithm.

HALOE and SAGE II do track each other very well. However it is very difficult to have lots of coincidences in both hemispheres within a month as compared to AIRS and MLS due to the limited measurements taken by HALOE and SAGE II. On the other hand, we do have at least a decade of data from both instruments and some of these measurements do go well into the upper troposphere. This has allowed us to get good enough coincidences between the two satellites and is both very useful data set specially in studying long term water vapor trends and time series.

Generally, these statistics are very comforting. Eliminating multiple coincidences did improve our statistics results. In cases where lot more data is available such as AIRS and MLS, tightening the Coincidence criteria's also improved the statistical outputs. In almost all the different sets of comparisons shown above the average differences tend to fall within the ± 50% Difference. The HALOE high HF bubble can be seen in many plots but not all and it tend to add a wet biasness to the HALOE averages. The recommended L2gpPrecission filter for the MLS data filters out lots of MLS measurements below the traupopause. Hence most of the MLS data stops at the 300Mbar level. Among the three sets of comparisons, it is hard to tell which pair yields the best results so far. However HALOE/SAGE II looks

very good and the measurements often go deeper into the upper troupposphere than HALOE/AIRS and HALOE/MLS.

Similar comparison between SAGE II/MLS, SAGE II/AIRS, and AIRS/MLS were also analyzed and can be seen in appendix B. While the SAGE II/MLS and SAGE II/AIRS plots looks very similar to the HALOE/MLS and HALOE/AIRS plots, the AIRS/MLS results yield a lot better result which we think is mainly due to the huge amount of data available from both instruments that made it possible to tighten the coincidence criteria from (±2Lat, ±12Lon, ±12hrs) to (±1Lat, ±1Lon, ±2hrs).

While these plots are very promising they are only monthly averages and hence are not conclusive enough to tell us how the data sets do compare seasonally or annually. It is also difficult to tell which instrument is drier or wet biased because the comparisons are only in pairs. In the next chapter, we intend to look at seasonal zonal mean plots and seasonal probability density functions of all four instruments simultaneously whenever possible.

CHAPTER 5

SEASONAL MEAN AND COMBINED LATITUDE PLOTS

This section comprises of two parts, one deals with seasonal zonal mean profiles of H_2O while the other deals with probability distribution functions (PDF) as an alternative way of comparing data sets.

5.1 Seasonal Zonal Means

With the seasonal zonal mean plots, we divided the globe into eight latitude bins, and for each seasonal latitude bin, we computed the mean profile for each instrument and plotted them as shown below. For each plot, the left hand side shows the overlayed seasonal mean profile plots with the percent difference relative to HALOE next to it. One advantage of these plots over those shown in the previous chapter is that plots are overlayed, hence we can easily see how each instrument compares seasonally with HALOE as well as with the other instruments. In addition, it is also easier to infer any seasonal dry or wet biasness within data sets if any. For each figure below, there are eight separate sets of plots, with a vertical line in the middle that separates the two hemispheres. For each plot, the one on the left shows the average

zonal mean profiles and the right shows the percent difference of each instrument relative to HALOE. The plots shown below were chosen out of many because they happened to have more data from all the instruments.

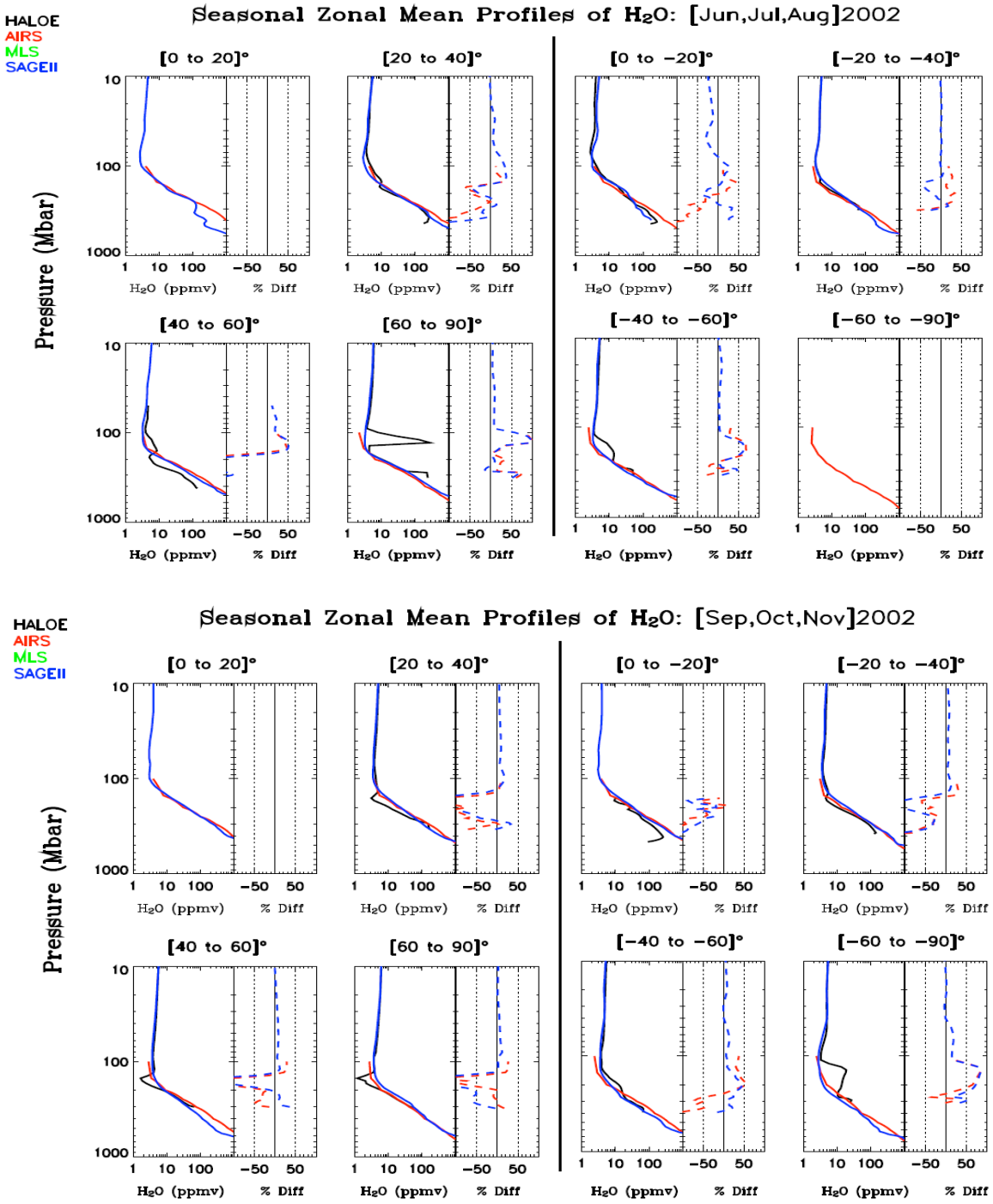

Figure: 5.1a (top) and Figure: 5.1b (bottom) seasonal zonal mean profiles for (Jun, Jul, Aug) and (Sep, Oct and Nov) 2002.

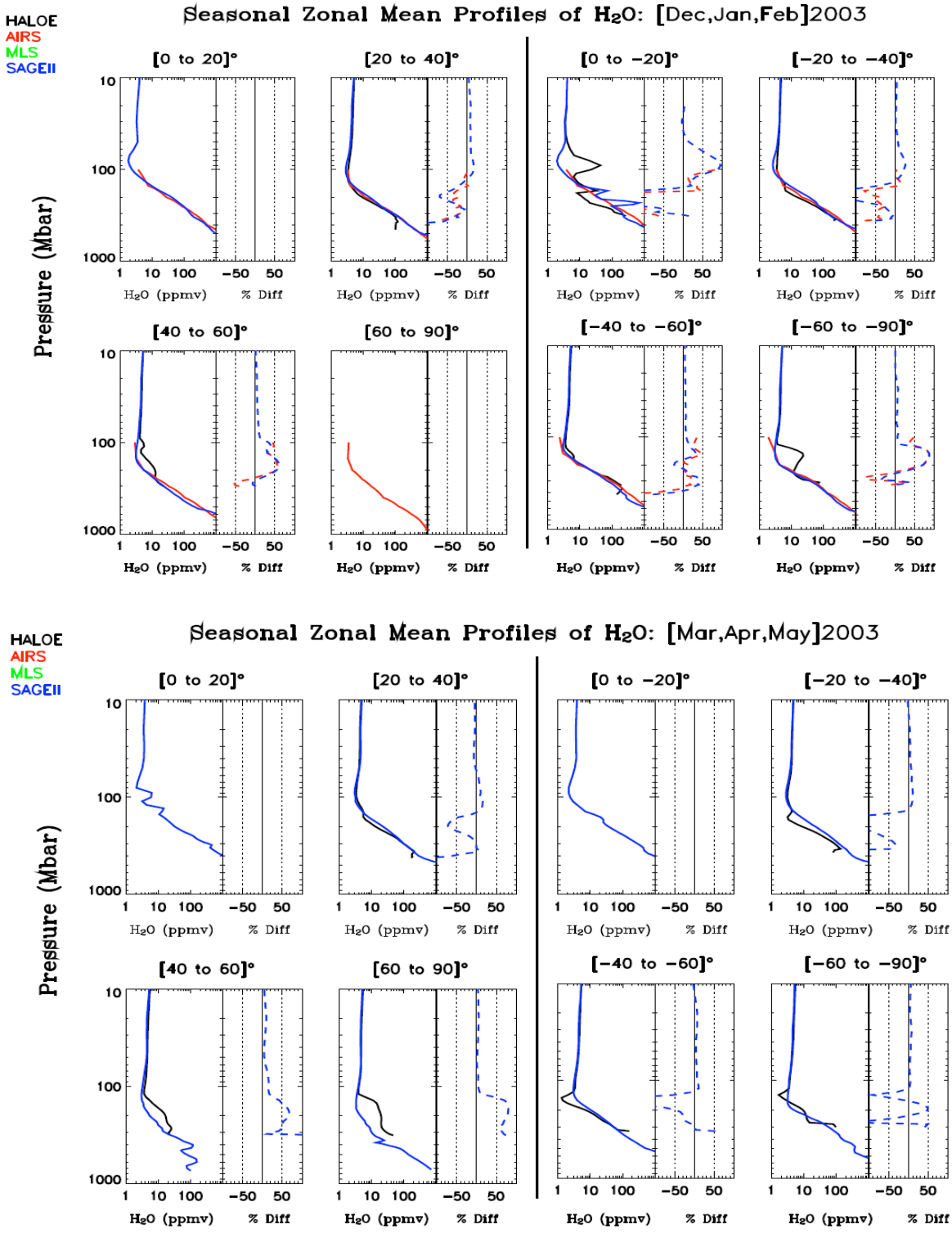

Figure: 5.1c (top) and Figure: 5.1d (bottom) seasonal zonal mean profiles for (Dec, Jan, Feb) and (Mar, Apr, May) 2003.

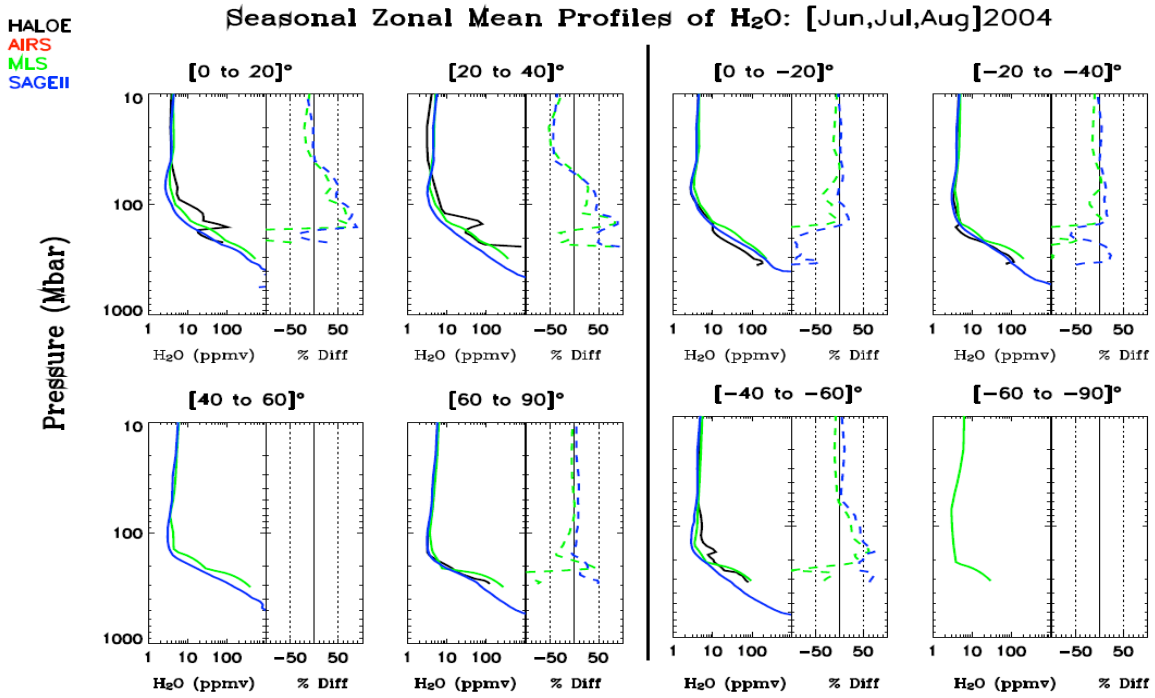

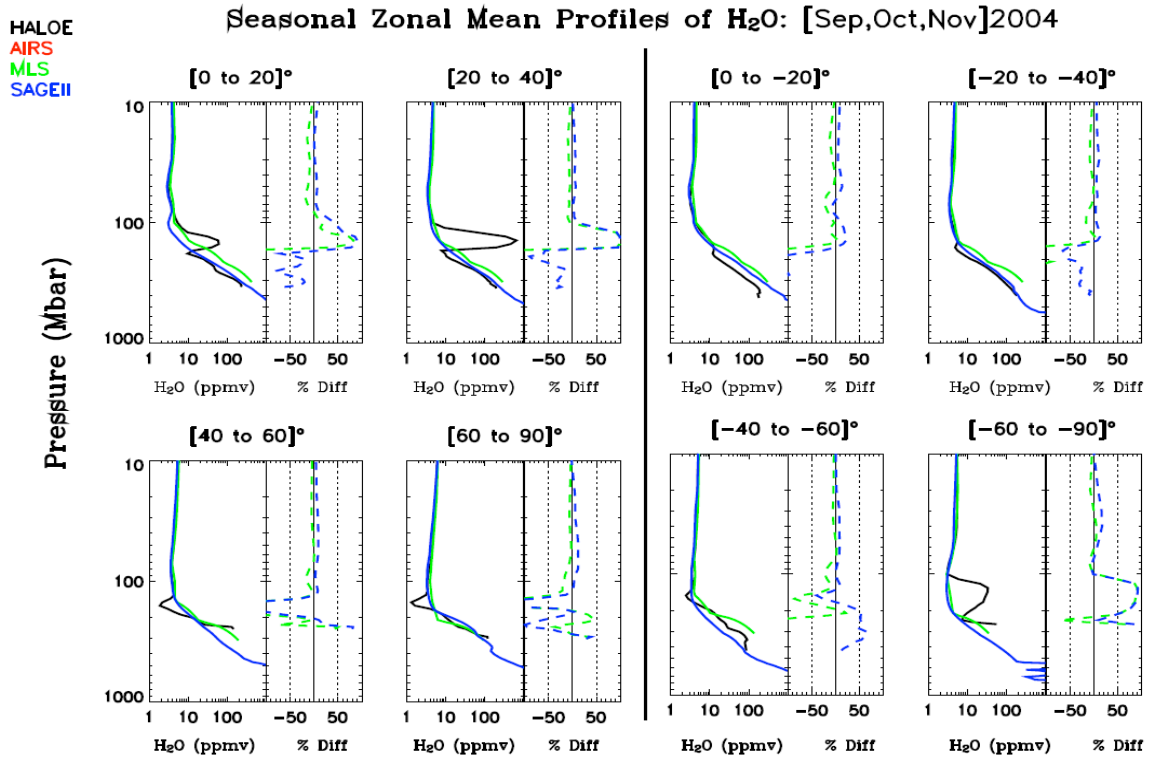

Figure: 5.1e (top) and Figure: 5.1f (bottom) seasonal zonal mean profiles for (Jun, Jul, Aug) and (Sep, Oct and Nov) 2004.

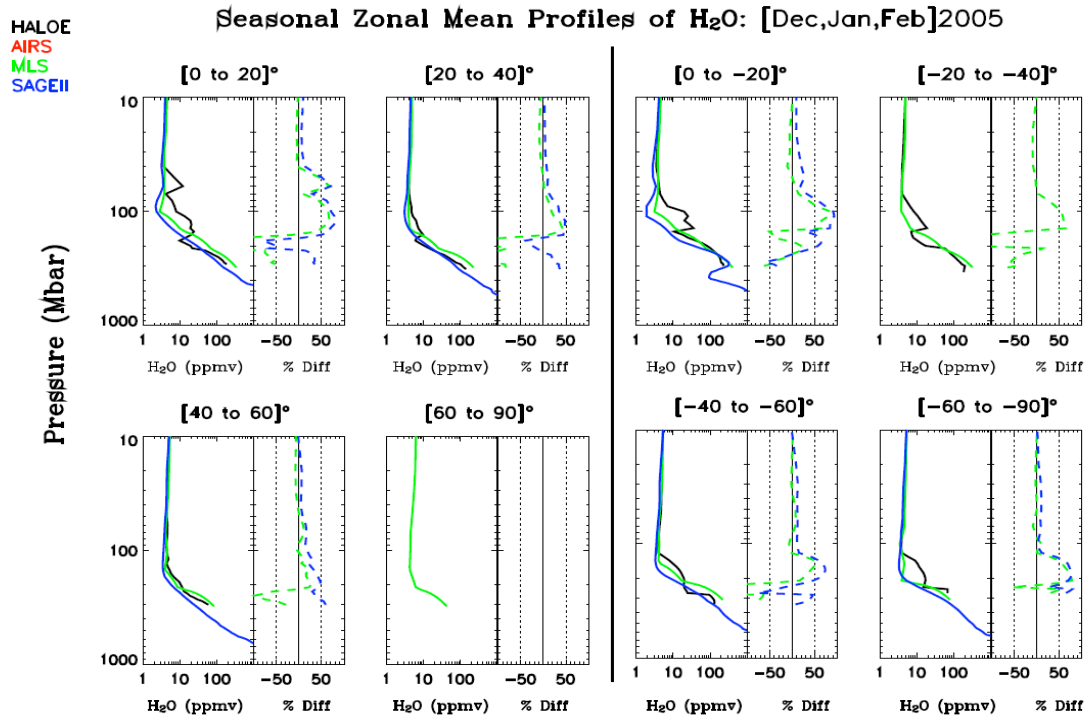

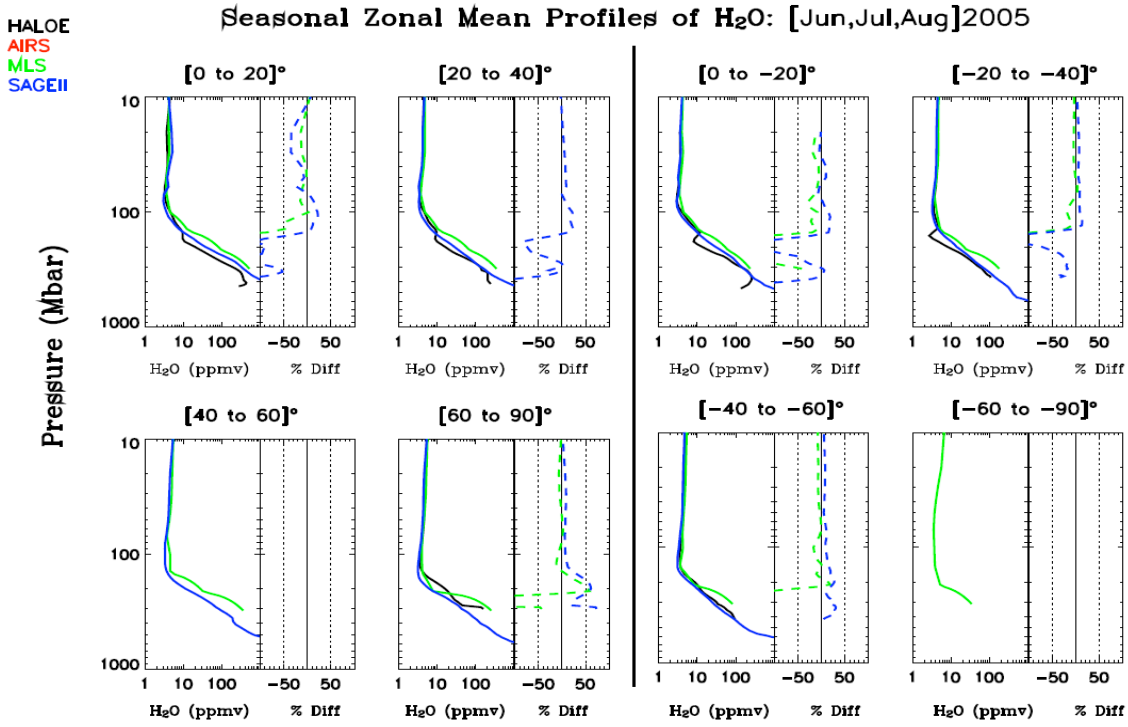

Figure: 5.1g (top) and Figure: 5.1h (bottom) seasonal zonal mean profiles for (Dec, Jan, Feb) and (Jun, Jul, Aug) 2005.

Generally(,?) there was no consistent relative dry or wet biasness across all latitudes for any one instrument over others. Just like the line-by-line comparisons and the monthly comparison plots, the seasonal zonal means also tend to fall within the ±50 % difference ranges if not even better. In some of the plots the high HF bubbles in HALOE V20 is very visible. Note that wherever HALOE data is not available in the plots above, the corresponding percent difference plot on the right hand is empty because for each instrument, the percent difference for the seasonal means were computed with respect to the corresponding HALOE seasonal mean. From these plots we can generally deduce that except for few exceptional cases, pressure ranges between [10 to 100mbars] all four instruments do fall within ±20 % difference and [100 to 1000mbars] do fall within ±50 % difference.

The high HF bubble can easily be seen in the [Jun, Jul, Aug] 2002 for the [60 to 90]° plot. SAGE II seems to agree very well with HALOE but so does HALOE-AIRS, with HALOE-MLS slightly behind these other sets. With these seasonal plots, we can easily deduce the fact that HALOE is slightly dry biased particularly in the upper trouposphere and below. However, there are also cases where HALOE is wet bias such as [Mar, Apr, May]- 2003 at [40 -60]° and [Dec, Jan, Feb]-2005at [40 – 60]° shown in the plots above. Hence, we can see that even though our statistics still shows some variability. Such result for lower stratosphere and higher traupospheric water vapor is very exciting and quiet promising.

With the limited date set we have and the importance of comparing unique events that are closest in position and time, it is very difficult to have huge amount of data that can yield very dependable statistical results even when the data sets are seasonally combine. In order to overcome this limiting barrier, additionally we did seasonally analyze our data sets using probability distribution functions (PDF) in the following section.

5.2 Probability Distribution Functions (PDF)

Probability distribution functions are an alternative way “to look at the overall fidelity” of datasets by comparing their (its?) “row probability distribution functions” (Gettelman, et al., 2005). Use of PDFs significantly aids comparisons of highly variable data reducing the importance of spectral coincidence. The

basic idea in PDF is to bin any given dataset not by measurements but rather by the number of times that measurements fall in a certain given ranger or bin size [say 20 to 30 ppmv]. The probability is then computed for each bin by dividing the count in that bin over the total counts in all the bins. A plot of these probabilities projected on the y-axis along with the mid point of each bin on the x-axis is what gave us our probability density plots shown below. In our case, we chose to seasonally bin the data and process only data that falls within the low and mid latitudes (-60 to 60) ° Latitude. In addition, only data that falls within the pressure range between 100-300mbar with H_2O values ranging between 10-1000 ppmv were used and subsequently grouped in 10ppmv wide size bins.

Even though PDF plots are computed separately for each data set and we do not have to worry much about setting coincidence criteria, we did find that where sufficient data is available, localizing data from each instrument can improve the quality and statistics of our plots. This is done by simply making sure that all the data from each instrument are reasonably close to those from the other instruments. Usually the closer the measurements the better the results, however this can be very tricky especially in our case because of the differences in the coverage ranges and the size of the data sets from the solar occultation and polar orbiting satellites.

The table below is a sample of seasonally binned data of HALOE, AIRS, MLS and SAGE II for the months of September, October and November of 2004 and within ±30° Latitude. The first column shows the 10° bins ranging from 1 to 1000 ppmv each centered at the middle. The following fours columns show the total counts from each instrument for each bin.

Due to the nature of our data, we decided to use a logarithmic scale. For each figure we have three plots divided into low, mid northern hemisphere and mid southern hemisphere latitudes. The y-axis represents the probability distributions ranging from (0 to1) and the x-axis represents the mean water vapor measurements ranging from (10 to 1000 ppmv). The small squares and triangles that are joined by the lines represent's mean measurement in each particular bin.

Probability Distribution function plots

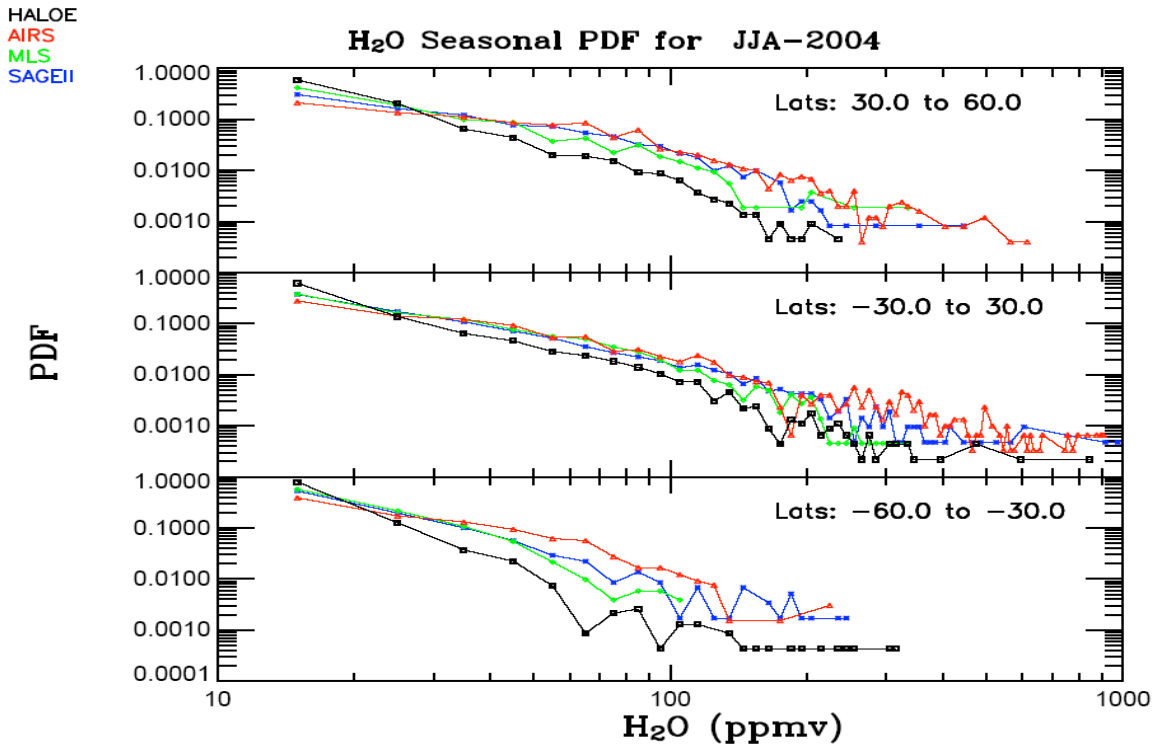

Figure: 5.2a Seasonal PDF for Jun, Jul and Aug of 2004.

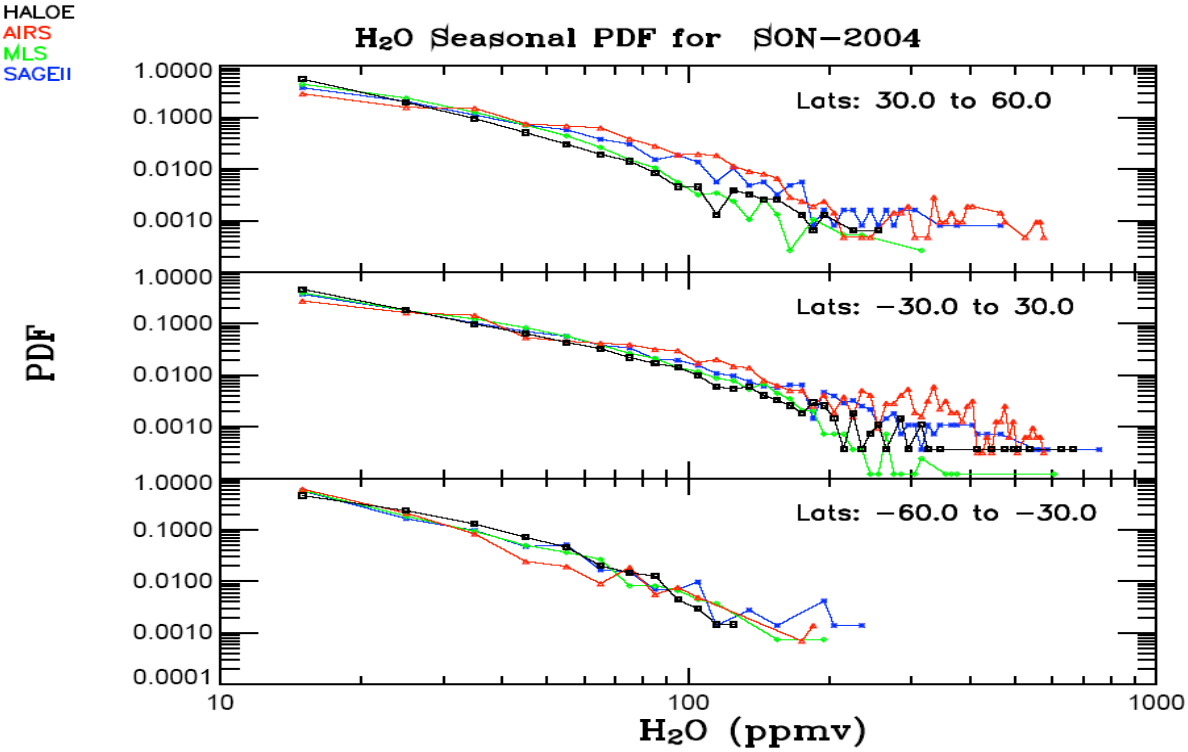

Figure: 5.2b (top) Seasonal PDF for Sep, Oct, Nov of 2004

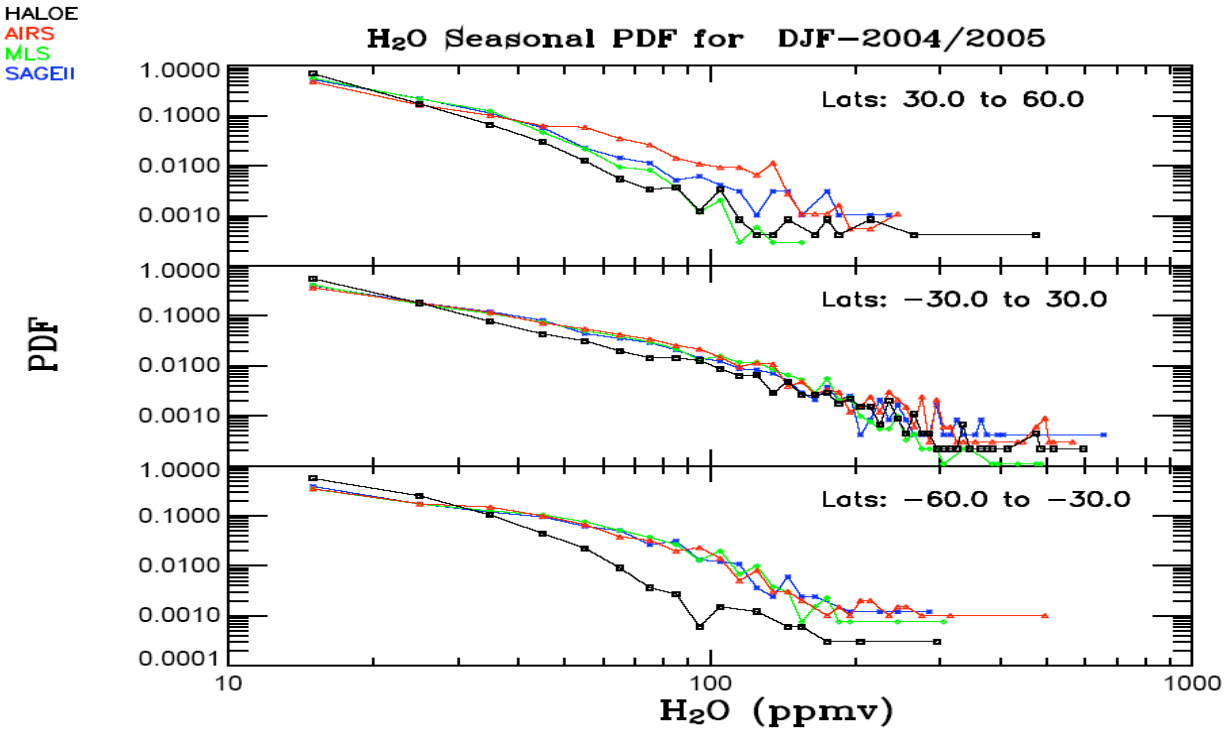

Figure: 5.2c . Seasonal PDF for Dec, Jan, Feb 2004/2005.

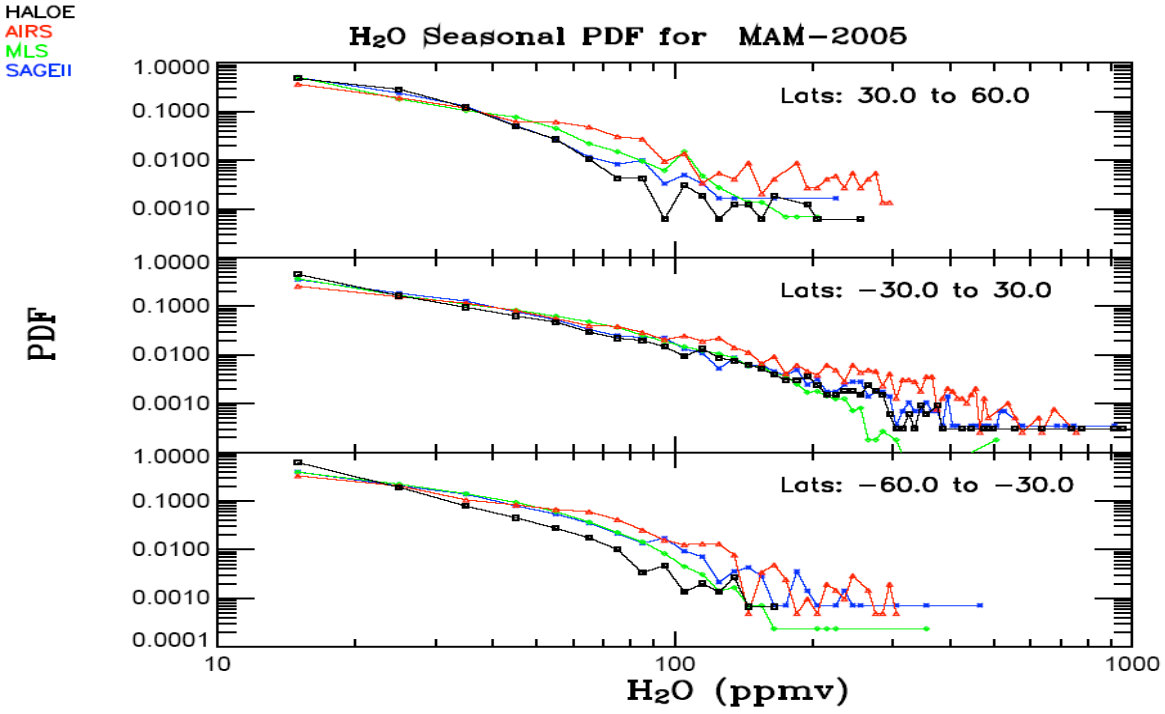

Figure: 5.2d (top) Seasonal PDF for Mar, Apr, May 2005.

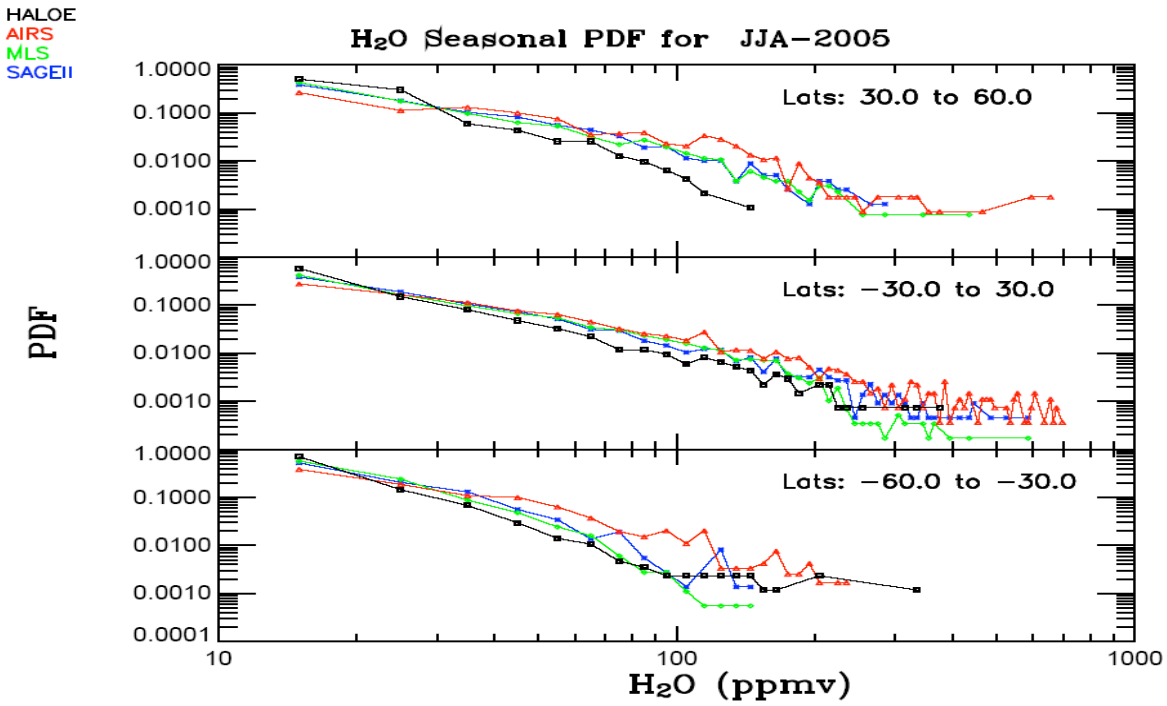

Figure: 5.2e Seasonal PDF for Jun, July, Aug 2005.

From the above PDF plots, we can generally conclude that these data sets are comparable. The comparisons look better between (1 to 100 ppmv), which corresponds to higher altitudes and often shows more variation between (100 to 1000ppmv). This is consistent with what we saw in our previous plots and it simply tells us that water vapor varies more as altitude decreases and you get closer to the earth's surface. We can also see that HALOE tends to start high in the fist bins and gradually gets lower as you move along the x-axis. While AIRS tends to start low in the lower bins and gradually gets relatively higher. This suggests a slight dry biasness for HALOE and a slight wet biasness for AIRS relative to the other instruments. In addition, we can also conclude from these plots that all the four instruments do agree better in the low latitudes (-30 to 30) ° than they do in the mid latitudes (-30 to 60) ° and (30 to 60) °. While these PDF plots have proven to be extremely helpful particularly in reducing the importance of spectral coincidences and providing us with an alternative means of comparing our data sets it is limited only into giving general information about how relatively wet or dry bias the data sets are. However it does not provide conclusive qualitative information about this relative dry or wet biasness. Hence to access this qualitative information, we decided to use an alternative plotting technique that allows us to combine all the

datasets from each instrument and group them into three general groups of (Low, Mid and High latitudes). This is an effort to summarize our findings with conclusive statistical values that will tell us how relatively dry or wet biased these instruments are.

5.3 Low, Mid and High Latitude combined plots

In this section, we are going to statistically show how HALOE compares relative to each correlative data set in the low, mid and high latitudes for all the coincidences found in the entire data set. This is done by searching for all the individual coincidences we could find between, HALOE-AIRS, HALOE-MLS, and HALOE-SAGE II, and dividing them into low, mid and high latitudes. We decided to combine the north and southern hemisphere's low latitudes together because of the limited amount of coincidences we found and the similarity between the two. Low, mid and high latitudes was defined as (±30) °, (±30 to ±60) ° and (±60 to ±90) ° respectively.

Just like the statistical comparison plots shown in chapter IV, for each set of plots, the top ones shows the spectral comparisons of the two data sets being compared in red and black with the total number of profiles and the covered latitude ranges. The plot below these spectral plots are the mean profiles plots of the two data sets on the left with the mean (mean of the differences) and the RMS % differences. The coincidence criterion was set to (±3° lat, ±12° lon, ±12hrs) and the horizontal lines shown on the mean plots represent standard error bars. The yellow shadings represent the taupopause range and the horizontal green line represents the mean traupopause height. For each HALOE profile, there is only one matching correlative profile, and where multiple correlative matches were found, we choose the one that is closest in latitude and time.

5.3.1 HALOE AND AIRS

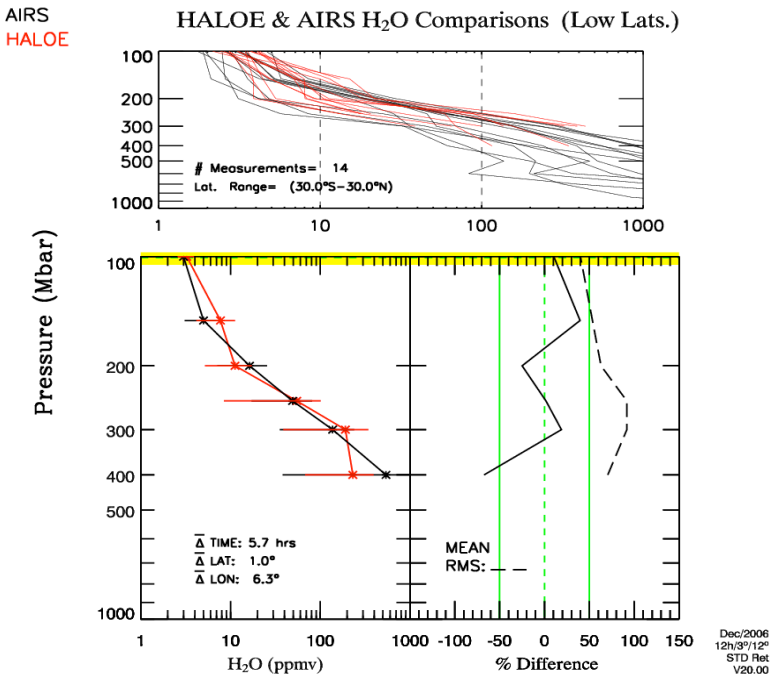

Figure: 5.3a HALOE/AIRS combined low latitudes.

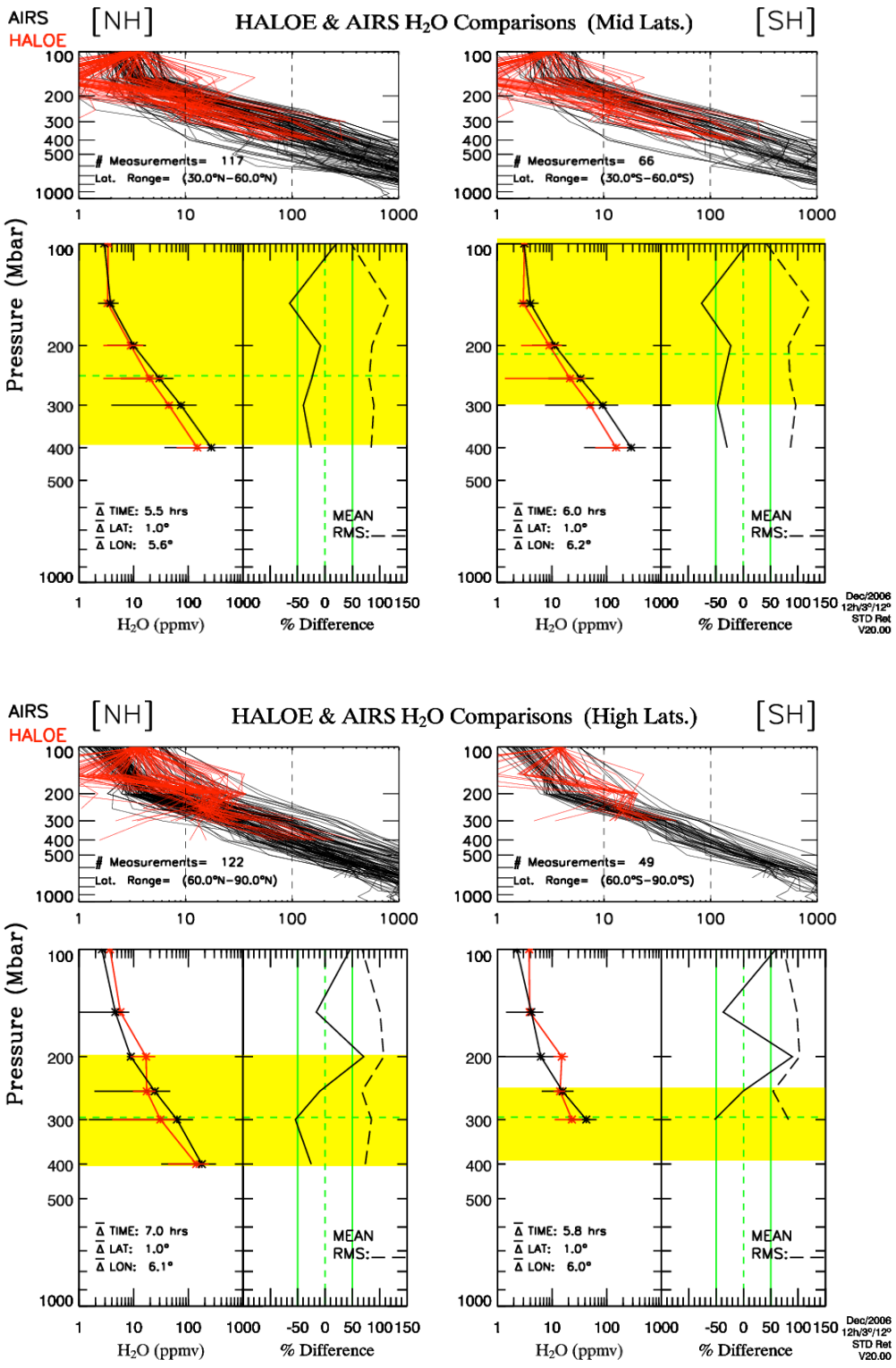

Figure: 5.3b (top) and Figure 5.3c (bottom) HALOE/AIRS combined mid and combined high latitudes respectively.

From the HALOE-AIRS comparison shown above we can generally deduce the following:

(I) Low latitudes: HALOE is wet biased over AIRS between the pressure ranges of ~(100- 180)mbar and ~(250 -310)mbar by ~ +20% differences, but dry biased between ~(180- 250)mbar and ~(310 -400)mbar by ~ -30% differences.

(ii) Mid latitudes: HALOE is dry bias over AIRS in the both hemispheres along all pressure levels by an average of ~ -30% difference except for between ~(100 -120)mbar where it slightly wet biased by ~ +10% difference. Note that this also happens to be the range with the largest amount of coincidences between the two instruments.

(iii) High latitudes: For the Northern hemisphere, HALOE is wet biased over AIRS between the pressure ranges of ~(100 -130)mbar and ~(160 -250)mbar by ~ +25% differences with a maximum wet biasness at 200mbar, but dry biased between ~(130- 160)mbar and ~(250 -400)mbar by ~ -30% differences.

5.3.2 HALOE AND MLS

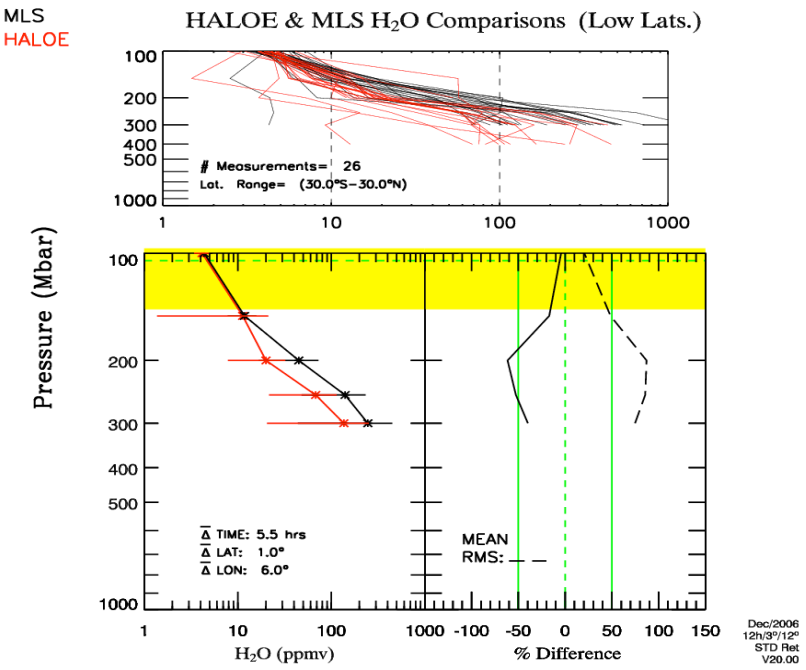

Figure: 5.4a HALOE/MLS combined low latitudes.

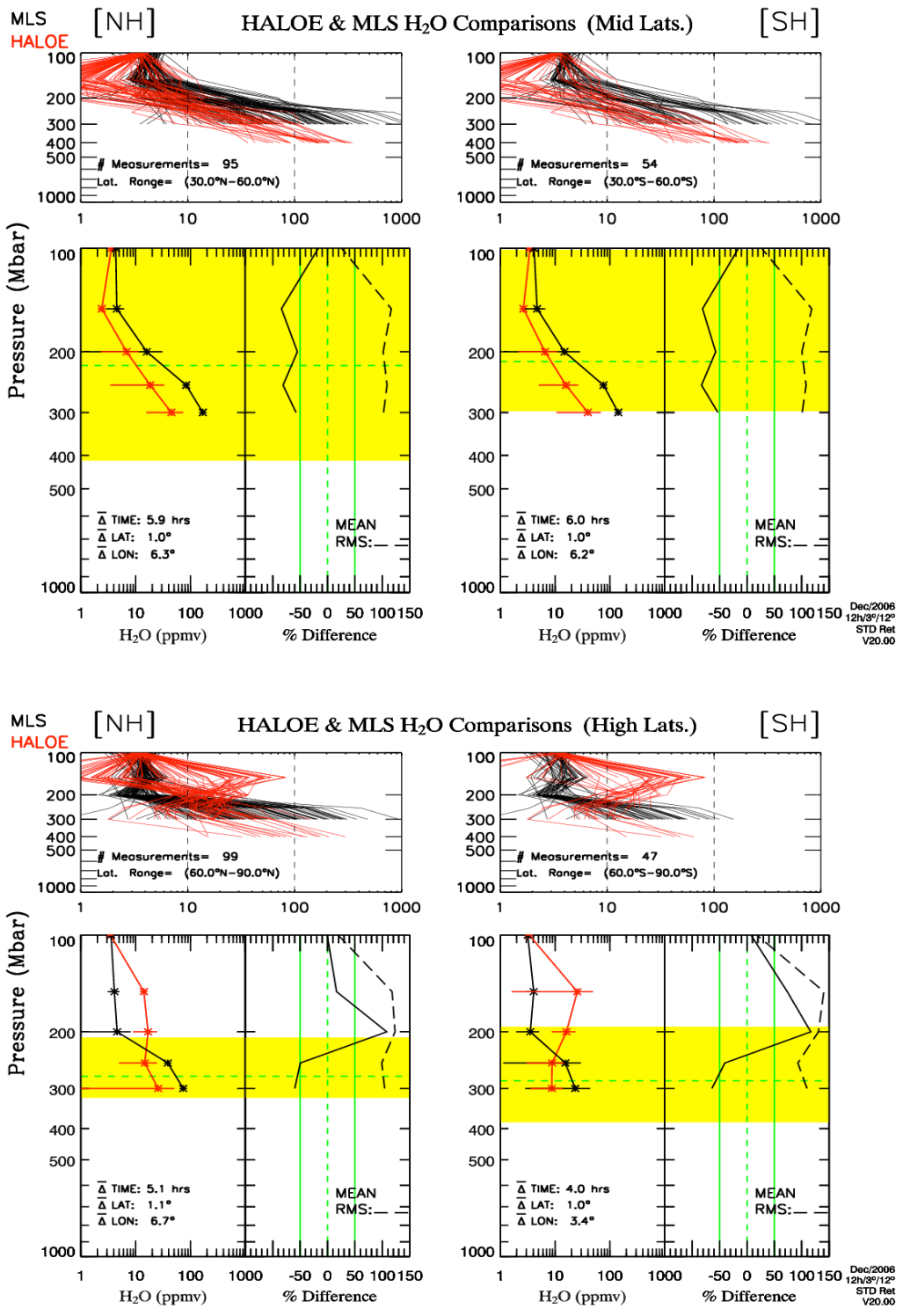

Figure: 5.4b (top) and Figure 5.4c (bottom) HALOE/MLS combined mid and combined high latitudes respectively.

From the HALOE-MLS comparison shown above we can generally deduce the following:

(I) Low latitudes: HALOE is dry biased over MLS for all pressure ranges in the lower latitudes by ~ -35% differences with maximum biasness being around 200mbar and the minimum at around 100mbar.

(ii) Mid latitudes: HALOE is dry biased over MLS in both hemispheres along all pressure levels by an average of ~ -50% differences. Maximum biasness is at the 150 and 250mbar marks and the minimum is at 100mbar.

(iii) High latitudes: HALOE is wet biased over MLS between the pressure ranges of ~ (100- 250) mbar by ~ +65% differences with a maximum biasness at 200mbar, but dry biased between ~ (250- 300) mbar by ~ -50% differences.

5.3.3 HALOE AND SAGE II

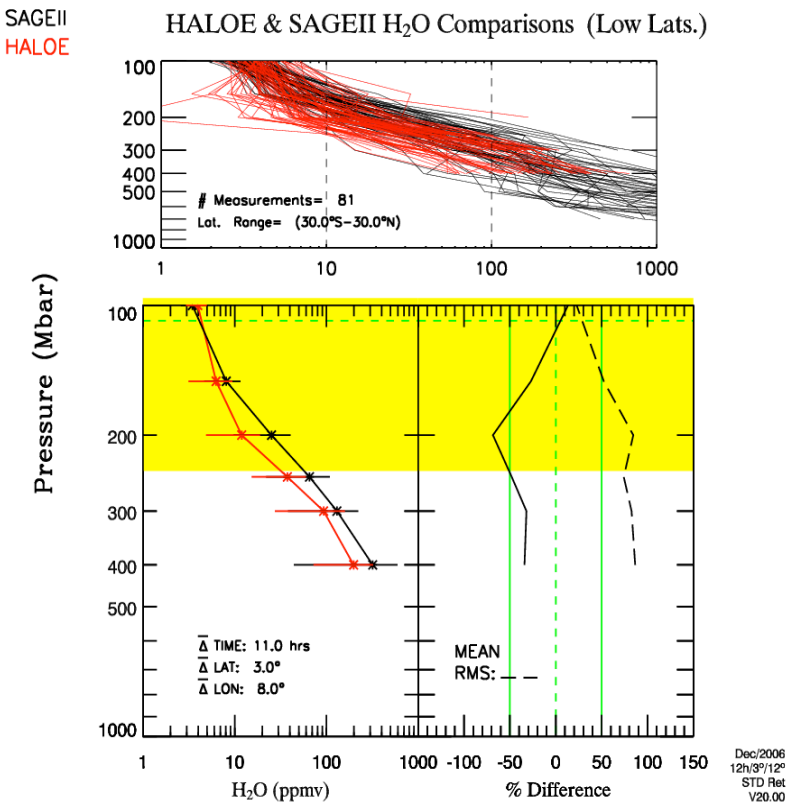

Figure: 5.5a HALOE/SAGE II combined low latitudes.

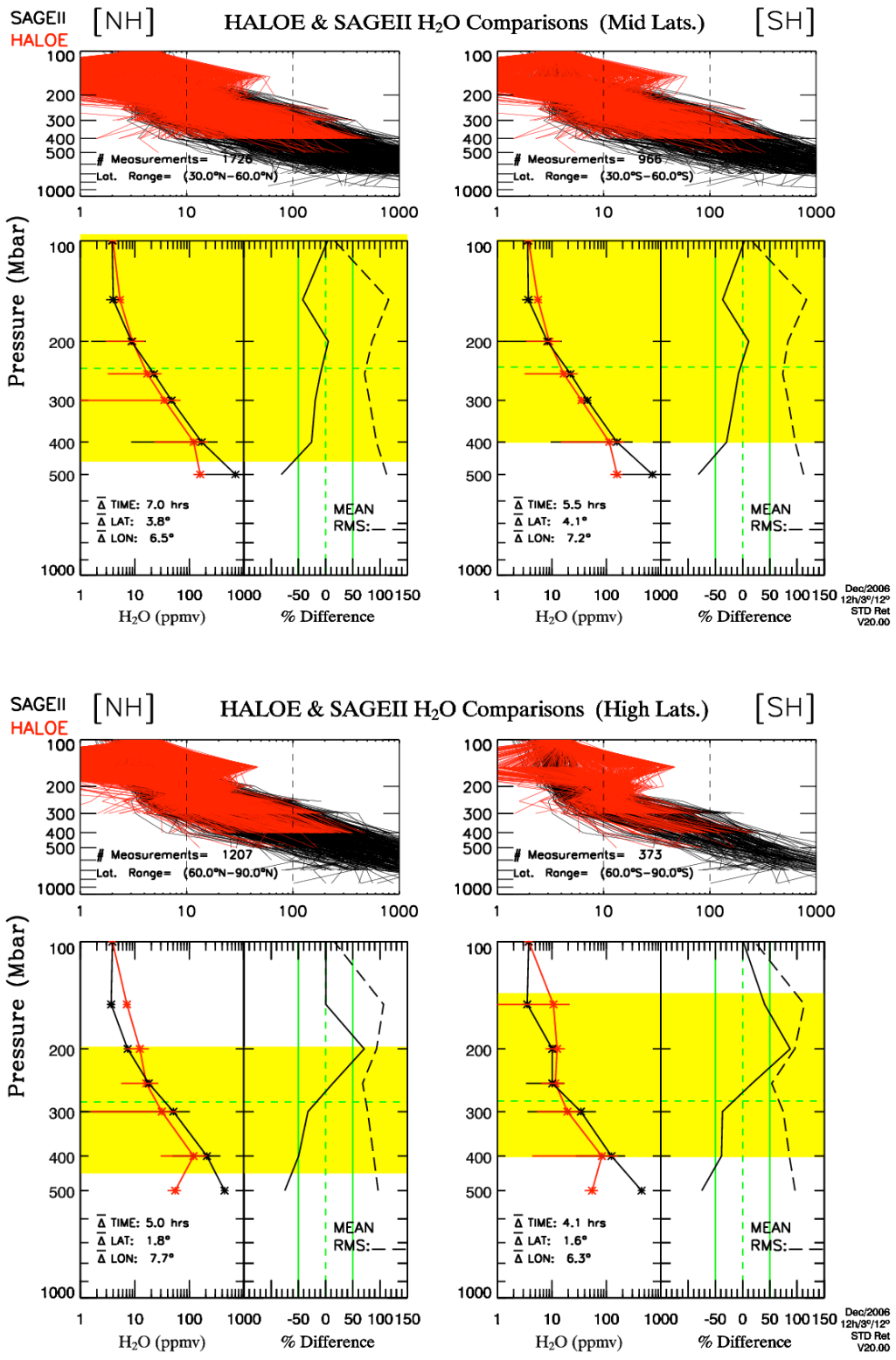

Figure: 5.5b (top) and Figure 5.5c (bottom) HALOE/SAGE II combined mid and combined high latitudes respectively.

From the HALOE-SAGE II comparison shown above we can generally deduce the following: (I) Low latitudes: HALOE is dry biased over SAGE II for all pressure ranges in the lower latitudes by ~ -40% differences, except at the 100mbar range where it is slightly wet biased by ~ +10% differences. (ii) Mid latitudes: HALOE is dry biased over SAGE II in both hemispheres along all pressure levels by an average of ~ -30% differences. However, it is worth noting that they are almost right on top of each other at 200mbar, which also happens to be the point with minimum % difference biasness for both hemispheres. (iii) High latitudes: HALOE is generally wet biased over SAGE II between the pressure ranges of ~ (100-250) mbar by ~ +35% differences with a maximum biasness at 200mbar, but dry biased between ~ (250-500) mbar by ~ -45% differences. Note how strikingly similar the north and southern hemisphere statistics looks despite large differences in the number of measurements that went into computing them. This can actually be seen in all the comparisons above. It suggests that the hemispheric biasness for a certain latitude range say the mid or high latitudes are very small if not negligible.

Now that we have found out the hemispheric differences are negligible, we combined both hemispheres and divided our entire data set into low, mid and high latitudes. In addition, we decided to overlay % difference for each instrument relative to HALOE so we can simultaneously see how all the instruments do compare, and these plots are shown in the next chapter.